

EUROPEAN ORGANISATION FOR NUCLEAR RESEARCH (CERN)



Submitted to: Physical Review C

CERN-PH-2015-146
November 10, 2015

Z boson production in $p+\text{Pb}$ collisions at $\sqrt{s_{NN}} = 5.02 \text{ TeV}$ measured with the ATLAS detector

The ATLAS Collaboration

Abstract

The ATLAS Collaboration has measured the inclusive production of Z bosons via their decays into electron and muon pairs in $p+\text{Pb}$ collisions at $\sqrt{s_{NN}} = 5.02 \text{ TeV}$ at the Large Hadron Collider. The measurements are made using data corresponding to integrated luminosities of 29.4 nb^{-1} and 28.1 nb^{-1} for $Z \rightarrow ee$ and $Z \rightarrow \mu\mu$, respectively. The results from the two channels are consistent and combined to obtain a cross section times the $Z \rightarrow \ell\ell$ branching ratio, integrated over the rapidity region $|y_Z^*| < 3.5$, of $139.8 \pm 4.8 \text{ (stat.)} \pm 6.2 \text{ (syst.)} \pm 3.8 \text{ (lumi.) nb}$. Differential cross sections are presented as functions of the Z boson rapidity and transverse momentum, and compared with models based on parton distributions both with and without nuclear corrections. The centrality dependence of Z boson production in $p+\text{Pb}$ collisions is measured and analyzed within the framework of a standard Glauber model and the model's extension for fluctuations of the underlying nucleon-nucleon scattering cross section.

Contents

1	Introduction	2
2	The ATLAS detector	3
3	Analysis	4
3.1	Data sample	4
3.2	Lepton reconstruction	4
3.3	Centrality	5
3.4	Monte Carlo simulation corrections	7
3.5	Yield extraction	8
3.6	Systematic uncertainties	10
3.7	Lepton channel combination	11
4	Results	12
4.1	$Z \rightarrow \ell\ell$ cross section	12
4.2	Centrality-dependent yield	14
5	Summary	18

1 Introduction

The study of electroweak bosons in Pb+Pb collisions at the Large Hadron Collider (LHC) at CERN has demonstrated that the production rate of non-strongly interacting particles scales with the number of nucleon-nucleon collisions, $\langle N_{\text{coll}} \rangle$. This has been observed for photons [1], W bosons [2, 3], and Z bosons [4, 5]. The momentum and rapidity distributions of Z boson yields are consistent with Pythia [6] simulations of $p p$ collisions multiplied by the average nuclear thickness function, $\langle T_{\text{AA}} \rangle$, which is equivalent to $\langle N_{\text{coll}} \rangle$ divided by the total nucleon-nucleon cross section [4]. Z boson production in Pb+Pb collisions was found to be consistent with Next to Leading Order perturbative Quantum Chromodynamics (NLO QCD) calculations that disregard nuclear modifications in the treatment of parton distribution functions (PDF). However, nuclear modification is not excluded within the precision of the measurement [7]. The production of Z bosons, when examined as a function of centrality, was also found to scale with $\langle N_{\text{coll}} \rangle$.

To differentiate between initial- and final-state effects in heavy ion (HI) collisions, the study of $p + \text{Pb}$ collisions is used at the LHC. One could expect that the hot and dense QCD medium cannot be formed in such collisions, unlike in the Pb+Pb case, and that modifications to the final-state particles relative to nucleon-nucleon collisions should originate from the initial state of the nucleus. This assumption was challenged by the very first results from $p + \text{Pb}$ collisions at $\sqrt{s_{\text{NN}}} = 5.02$ TeV produced at the LHC in 2012. Results on multi-particle correlations, published by three LHC experiments [8–14], revealed collective behavior in $p + \text{Pb}$ collisions similar to that previously measured in HI collision systems. The yields of jets measured by ATLAS scale with $\langle N_{\text{coll}} \rangle$ when measured inclusively for all centralities, but show significant deviations from binary scaling when considered in centrality selections [15]. The CMS Collaboration has measured dijet pseudorapidity distributions and found them to agree better with predictions that include nuclear PDF modifications than with predictions that do not include nuclear effects [16]. The CMS Collaboration has also recently measured production of W bosons in $p + \text{Pb}$ collisions and

observed hints of nuclear modifications of the PDF [17]. Collectively, these results have highlighted the need for a better understanding of the initial conditions of $p+\text{Pb}$ collisions.

Unlike symmetric $\text{Pb}+\text{Pb}$ collisions, in $p+\text{Pb}$ collisions nuclear modifications of the PDFs in the lead nucleus create an asymmetry in the rapidity-dependent cross section of Z bosons; this presents an attractive observable for the study of initial-state nuclear conditions. The centrality-dependent yield of Z bosons is a well suited probe to test our understanding of $p+\text{Pb}$ collision geometry. The LHCb Collaboration has made a first exploratory measurement of Z bosons at far forward and backward rapidities [18] based on an integrated luminosity of 1.6 nb^{-1} .

This paper presents the results of the measurement of Z boson production in $p+\text{Pb}$ collisions at $\sqrt{s_{NN}} = 5.02 \text{ TeV}$ using the ATLAS detector. The yield of Z bosons is measured as a function of their transverse momentum p_T^Z , rapidity in the center-of-mass frame (y_Z^*),¹ and centrality. The leptonic decays of the Z boson ($Z \rightarrow ee$ and $Z \rightarrow \mu\mu$) are used for its reconstruction. In the muon channel it is possible to reconstruct the Z boson in the rapidity range $-3 < y_Z^* < 2$, while in the electron channel this range can be extended to $|y_Z^*| < 3.5$. The larger acceptance in rapidity for $Z \rightarrow ee$ candidates is possible because of the larger acceptance of the ATLAS calorimeters compared to the muon spectrometer (MS; Secs. 2 and 3.2). The efficiency of Z boson reconstruction is calculated from detector simulations (Sec. 3.4). Backgrounds in each channel are estimated using simulations and data-driven methods (Sec. 3.5). Results measured in the dimuon and dielectron decay channels are combined after accounting for uncertainties and their correlations (Sec. 3.7). The measured cross sections and centrality-dependent yields are compared to models of $p+\text{Pb}$ collisions composed of 82 pp and 126 pn collisions in which the production of Z bosons is obtained using perturbative QCD calculations.

2 The ATLAS detector

The ATLAS detector [19] at the LHC covers nearly the entire solid angle around the collision point. It consists of an inner tracking detector surrounded by a thin superconducting solenoid, electromagnetic and hadronic calorimeters, and the MS.

The inner-detector (ID) system is immersed in a 2 T axial magnetic field and provides charged particle tracking in the pseudorapidity range $|\eta| < 2.5$. It comprises a high-granularity silicon pixel detector covering the collision region, surrounded by a silicon microstrip tracker and a transition radiation tracker.

The calorimeters cover the range $|\eta| < 4.9$. Within the region $|\eta| < 3.2$, electromagnetic calorimetry is provided by barrel and endcap high-granularity lead liquid-argon (LAr) calorimeters, with an additional thin LAr presampler covering $|\eta| < 1.8$. Behind the electromagnetic calorimeter there is a steel/scintillator sampling hadronic calorimeter covering $|\eta| < 1.7$, and LAr hadronic calorimeters extend the coverage to $|\eta| < 4.9$. Forward electromagnetic calorimeters (FCals) are located in the range $3.1 < |\eta| < 4.9$. Electrons may be reconstructed over the entire electromagnetic calorimeter system, $|\eta| < 4.9$.

¹ ATLAS uses a right-handed coordinate system with its origin at the nominal interaction point (IP) in the center of the detector and the z -axis along the beam pipe. The x -axis points from the IP to the center of the LHC ring, and the y -axis points upward. Cylindrical coordinates (r, ϕ) are used in the transverse plane, ϕ being the azimuthal angle around the beam pipe. The rapidity in the laboratory frame is given by $y^{\text{lab}} = \frac{1}{2} \ln \frac{E+p_z}{E-p_z}$ and pseudorapidity is defined as $\eta = -\ln[\tan(\theta/2)]$. Positive rapidity corresponds to the direction the proton beam travels, “proton-going”, and negative rapidity is referred to as “Pb-going”. In this convention the asymmetric beam energies result in a center-of-mass shifted to rapidity $y^* = y^{\text{lab}} - 0.465$.

The MS comprises separate trigger and high-precision tracking chambers that measure the deflection of muons in a magnetic field generated by superconducting air-core toroids. The precision chambers cover the region $|\eta| < 2.7$ with three layers of monitored drift tubes (MDT) chambers, complemented by cathode strip chambers (CSC) in the innermost layer of the forward region. The muon trigger system covers the range $|\eta| < 2.4$ with resistive plate chambers (RPC) in the barrel ($|\eta| < 1.05$), and thin gap chambers (TGC) in the endcap regions ($1.05 < |\eta| < 2.4$).

The ATLAS detector has a three-level trigger system [20]: the hardware-based level-1 (L1) trigger and the software-based High Level Trigger (HLT), which is subdivided into the Level-2 (L2) trigger and Event Filter (EF). Single-electron and single-muon triggers are used to acquire the data analyzed in this paper. Minimum-bias events are selected based on signals in the minimum-bias trigger scintillators (MBTS) that detect charged particles in the range $2.1 < |\eta| < 3.9$.

3 Analysis

3.1 Data sample

This analysis uses the 2013 ATLAS p +Pb collision data at $\sqrt{s_{NN}} = 5.02$ TeV, produced from a 4 TeV proton beam and a 1.57 TeV per nucleon lead beam. The asymmetric energy of the beams resulted in a shift of the center-of-mass by 0.465 units of rapidity relative to the laboratory frame. After 60% of the data were recorded the directions of the proton and lead beams were reversed. Results obtained in the two data periods are found to be consistent with each other. In this paper all data from both periods are presented using the convention that the proton beam travels *forward* in the positive rapidity direction.

Following stringent data-quality requirements, the $Z \rightarrow ee$ and $Z \rightarrow \mu\mu$ analyses use samples corresponding to integrated luminosity values of $29.4 \pm 0.8 \text{ nb}^{-1}$ and $28.1 \pm 0.8 \text{ nb}^{-1}$, respectively. The luminosity measurement for the 2013 p +Pb data is calibrated based on dedicated beam-separation scans. Systematic uncertainties similar to those studied for the calculation of pp luminosity [21] are calculated. The combination of these systematic uncertainties results in a total uncertainty in the ATLAS luminosity scale during proton-lead collisions at $\sqrt{s_{NN}} = 5.02$ TeV of 2.7%. Minimum-bias p +Pb collisions were selected by a trigger based on a signal in both MBTS counters. Minimum-bias events are required to have the time measured in each MBTS be consistent within 10 ns, and a reconstructed collision vertex within 175 mm of the nominal collision point in the longitudinal direction [22].

3.2 Lepton reconstruction

Electron candidates are first identified by the L1 trigger as a cluster of cells in the electromagnetic calorimeter, formed into $(\Delta\phi \times \Delta\eta) = 0.1 \times 0.1$ trigger towers, within the range $|\eta| < 2.5$ and with the cluster transverse energy exceeding 5 GeV. The HLT then incorporates tracking information from the ID and imposes electron identification requirements on the electron candidates. A trigger for at least one electron candidate with $E_T > 15$ GeV and satisfying loose identification requirements is used to select events.

In the offline analysis, electron candidates within $|\eta| < 4.9$ are selected using the ATLAS reconstruction algorithm [23]. Electrons with $|\eta| < 2.47$, referred to as midrapidity electrons, require the matching of

a track to an energy cluster in the electromagnetic calorimeter. In addition to the reconstruction requirements, further electron identification selections based primarily on the shower shape in the electromagnetic calorimeter are made to reject background. Electron identification requirements used in previous ATLAS analyses [23] are used to provide quality classification of electrons based on the tightness of the identification criteria they satisfy. The triggering electron is required to have $E_T > 20$ GeV, to be outside the pseudorapidity interval $1.37 < |\eta| < 1.52$ (a transition region between the barrel and endcap calorimeters which contains a relatively large amount of inactive material), and to satisfy tight identification quality requirements. If the other electron is within $|\eta| < 2.47$, it must have $E_T > 10$ GeV and satisfy looser quality requirements. Forward-electrons are those reconstructed within the range $2.5 < |\eta| < 4.9$ based on energy deposited in the FCal [23]. There is no tracking in this region, so the electron candidate reconstruction and identification is derived solely from the calorimeter signal and does not have an associated charge. Forward-electrons are required to have $E_T > 20$ GeV. Of $Z \rightarrow ee$ decays with $|y_Z^*| < 3.5$, approximately 82% fall into the fiducial acceptance defined by the electron p_T and η requirements.

Muon candidates are first identified at the L1 trigger, based on hits in either the RPC or TGC. The HLT then reconstructs muon tracks in the vicinity of the detector region reported by the L1 trigger. The L2 trigger uses an algorithm to perform a fast reconstruction of muons, which is then refined in the EF by incorporating the hits in the ID tracking as well as those in the MS tracking. Events containing at least one muon with p_T greater than 8 GeV are accepted by the HLT.

For the $Z \rightarrow \mu\mu$ analysis, muons are identified from candidates reconstructed in both the MS and ID [24]. Muons are reconstructed separately in the MS and ID and a χ^2 -minimization procedure is used to obtain combined muon kinematic information. To reduce background from jets, each muon is required to pass a loose track-based isolation selection. Tracks are considered in a cone of size $\Delta R = \sqrt{(\Delta\eta)^2 + (\Delta\phi)^2} = 0.3$ around the direction of the muon. The muon is considered isolated if the scalar sum of the p_T of these tracks, excluding the muon, is less than 50% of the muon p_T . The efficiency of this selection is greater than 99%. The triggering muon is required to have $p_T > 20$ GeV and be within $|\eta| < 2.4$. The second muon must be within $|\eta| < 2.47$ and have $p_T > 10$ GeV. Approximately 68% of Z bosons with $-3 < y_Z^* < 2$ fall into the fiducial acceptance defined by the muon kinematic requirements.

3.3 Centrality

In addition to measuring the Z boson cross section, the Z boson yield per minimum-bias event is measured for different centrality selections. In order to characterize the p +Pb collision geometry, each event is assigned a centrality based on the total transverse energy measured in the FCal on the Pb-going side ($-4.9 < \eta < -3.2$), ΣE_T^{FCal} [22]. Collisions with more (fewer) participating nucleons are referred to as central (peripheral). As in Ref. [22], the standard Glauber model [25] approach is used to calculate the mean number of participating nucleons, $\langle N_{\text{part}} \rangle$. The mean number of inelastic nucleon-nucleon collisions, $\langle N_{\text{coll}} \rangle$, is $\langle N_{\text{part}} \rangle - 1$. Based on the observed centrality dependence of the charged particle multiplicity [22], a Glauber-Gribov Color Fluctuation (GGCF) model [26, 27], an extension to the Glauber model which allows event-by-event fluctuations of the nucleon-nucleon cross section $\sigma(N + N \rightarrow X)$, is also considered. In this model the magnitude of the fluctuations is characterized by the parameter ω_σ , with $\omega_\sigma=0$ corresponding to the standard Glauber model. Following Ref. [22], two values of ω_σ , 0.11 and 0.2, based on the calculations in Refs. [26, 27], are implemented and considered for this analysis.

Following Ref. [22], the centrality selections used for this analysis, in order from most central to most peripheral, are 0–5%, 5–10%, 10–20%, 20–30%, 30–40%, 40–60%, and 60–90%. For the study of the

y_Z^* distribution as a function of centrality (see Sec. 4.2), larger bins are used: 0–10%, 10–40%, and 40–90%. For the most peripheral collisions, centrality greater than 90%, centrality modeling, and associated geometric quantities are not well constrained. Pileup events, those containing multiple p +Pb interactions from the same bunch-crossing, are removed by rejecting events in which more than one primary vertex is reconstructed. The fraction of candidate events which is removed from the centrality-selected Z boson yield analysis due to pileup rejection is approximately 5%. Diffractive events are identified by a rapidity gap (defined by the absence of calorimeter energy clusters) of greater than two units on the Pb-going side of the detector, and excluded. This leads to a rejection of less than 0.1% of Z boson candidate events. The total number of minimum-bias events corresponding to the luminosity sampled by the trigger, N_{evt} , is used to define the Z boson yield per event in each centrality selection.

Besides its sensitivity to the event geometry, the $\Sigma E_{\text{T}}^{\text{FCal}}$ for a fixed geometry may also be affected by the presence of a hard scattering process in the event. In particular, the calculation of centrality for $Z \rightarrow ee$ events in which there is a forward-electron in the Pb-going side FCal, is biased by the energy of the electron. This is corrected by subtracting the transverse energy of the electron from $\Sigma E_{\text{T}}^{\text{FCal}}$. The subtraction procedure is found to effectively recover the correct centrality of minimum-bias events into which simulated $Z \rightarrow ee$ decays containing electrons in the Pb-going side FCal were overlaid.

In addition to the case where there is a Z -decay electron in the Pb-going side FCal, $\Sigma E_{\text{T}}^{\text{FCal}}$ may be more subtly biased in all Z boson events. The presence of a Z boson (or any hard process) is correlated with a higher transverse energy of the underlying event. Consequently, more energy may be deposited in the Pb-going side FCal in events containing a hard scattering process than in those that do not contain one. This causes a bias in the centrality-dependent yield, as the Z boson yield is enhanced in the more central events but depleted in the more peripheral ones. This effect, referred to as a centrality bias, has been noted for yields of hard processes in d +Au collisions at $\sqrt{s_{\text{NN}}} = 200$ GeV by the PHENIX Collaboration [28], and by the ALICE Collaboration in p +Pb collisions at $\sqrt{s_{\text{NN}}} = 5.02$ TeV by the ALICE Collaboration [29].

A correction to the centrality-dependent yields of hard processes in d +Au collisions at $\sqrt{s_{\text{NN}}} = 200$ GeV has been studied by the PHENIX Collaboration [28] (the correction is also calculated for p +Pb at $\sqrt{s_{\text{NN}}} = 5.02$ TeV). The centrality bias correction used by the PHENIX Collaboration is based on the modeling of an increase in the mean particle multiplicity produced by the specific NN collision that undergoes a hard scattering. Recently, similar calculations of a centrality bias have been made in which all NN collisions may contribute to an increase in the particle multiplicity [30]. The increase in multiplicity stemming from each NN collision is taken to be proportional to the contribution from that collision to the E_{T} in the event. This model is applied to the ATLAS p +Pb centrality classification for the standard Glauber analysis as well as the GGCF models, and thus used to calculate corrections to the hard process yield measured in a given centrality bin. Because the N_{part} probability distribution varies less steeply in the GGCF models than in the standard Glauber model, the centrality bias corrections are closer to unity for the GGCF cases. The corrections from Ref. [30] are shown in Figure 1. The reciprocals of the corrections are applied as multiplicative factors to the centrality-dependent Z boson yields measured in the present analysis.

Using Z bosons measured in ATLAS, data-driven centrality bias corrections may be calculated and compared with the results from Ref. [30]. To do so, the corrections are calculated by comparing the transverse energy deposited in the FCal in events selected by the minimum-bias trigger and in Z boson events from pp collisions (in which there is no centrality to consider). This effect is studied in pp collisions at $\sqrt{s} = 2.76$ TeV and $\sqrt{s} = 7$ TeV from the 2011 LHC run. At both energies a significant increase in the mean transverse energy deposited in the FCal is observed, and within the uncertainties of the measurement found to be independent of the Z boson kinematics. A single value is interpolated from the

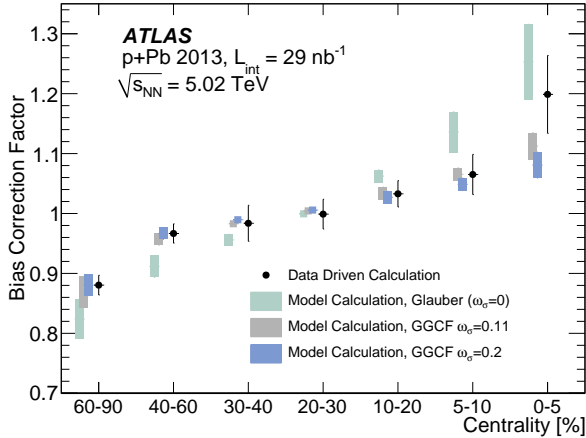


Figure 1: (Color online) Centrality bias correction factors and their uncertainties (bars), from Ref. [30], for the Glauber and GGCF model configurations, and the bias correction factors derived from data (points) as explained in the text. The reciprocals of the correction factors are applied as multiplicative factors to the centrality-dependent Z boson yields.

$\sqrt{s} = 2.76$ TeV and $\sqrt{s} = 7$ TeV data for $\sqrt{s_{NN}} = 5.02$ TeV. The interpolation is performed using both logarithmic and linear expressions, and the difference between them contributes to the systematic uncertainty. A correction is made to account for the shifted center-of-mass in the p +Pb system which changes the effective FCal acceptance in η compared to pp . From this procedure an additive shift to ΣE_T^{FCal} of 2.0 ± 0.5 GeV is calculated. In each p +Pb $Z \rightarrow \ell\ell$ event this value is subtracted from ΣE_T^{FCal} and the resulting value used to determine a corrected centrality of the event. The centrality-dependent yield may be constructed, according to the method described in Sec. 3.5, using both the subtracted and unsubtracted ΣE_T^{FCal} values and their ratio is then comparable to a centrality bias correction factor that may be compared to those calculated in Ref. [30]. As shown in Figure 1, within the uncertainties this data-based method is compatible with the model calculations.

3.4 Monte Carlo simulation corrections

The trigger, reconstruction, and identification efficiencies of electrons and muons as well as the muon isolation efficiency are evaluated by a Monte Carlo (MC) simulation complemented by data-driven estimates of these quantities. Using the PowHEG generator [31] (with the CT10 PDF [32]) interfaced to PYTHIA8 [6] for simulation of the parton shower, approximately 10 million $Z \rightarrow ee$ and 4 million $Z \rightarrow \mu\mu$ events were simulated. The Z bosons were generated from pp and pn collisions, which were added together with weights 82/208 and 126/208, respectively, corresponding to the numbers of protons and neutrons in the Pb ion. The response of the ATLAS detector to the generated particles was modeled using GEANT4 [33, 34]. Due to the dependence of electron identification and reconstruction efficiency on detector occupancy, the simulated $Z \rightarrow ee$ events were overlaid with data events selected with the minimum-bias trigger, and then reconstructed.

To cross-check the efficiencies calculated in the MC simulation, a ‘tag-and-probe’ technique is employed. A ‘tag’ is defined as a fully reconstructed high-quality triggered lepton, whereas the ‘probe’ is a lepton candidate to which triggering, reconstruction, or quality requirements are not applied. Using tag-and-probe pairs with an invariant mass $m_{\ell\ell}$ consistent with selection of Z bosons, the efficiency of the probe

with additional requirements is calculated. The mass window used depends on the background present in the probe sample, and ranges from $80 < m_{\ell\ell} < 100$ GeV to $87 < m_{\ell\ell} < 95$ GeV. For example, the electron trigger efficiency is measured from high-quality reconstructed electron probes selected without an *a priori* trigger requirement, and the MS reconstruction efficiency is measured from charged-particle tracks in the ID without an *a priori* MS signal requirement. The MC simulation is scaled to match the efficiencies determined with the data-driven tag-and-probe method. The factors used to scale the MC electron response are derived from the 2013 $p+\text{Pb}$ data set. Muon reconstruction is insensitive to the differences between 2013 $p+\text{Pb}$ and 2012 pp conditions and therefore the scale factors for muons are taken from $Z \rightarrow \mu\mu$ events collected in the 2012 pp dataset [24]. The scale factors for the $Z \rightarrow ee$ ($Z \rightarrow \mu\mu$) MC events deviate from unity by less than 5% (1%).

The trigger efficiencies of electrons and muons depend on η , and have average values of approximately 95% and 83%, respectively. The reconstruction and identification efficiency of the more stringently selected electrons is approximately 75%, whereas the reconstruction and identification efficiency for the looser-quality midrapidity electrons is approximately 88% and the forward-electron efficiency is about 65%. These values depend on η and p_T . The muon reconstruction efficiency is approximately 95%, depending on η .

Correction factors for the yields of $Z \rightarrow ee$ and $Z \rightarrow \mu\mu$ candidates are calculated from the MC simulations as functions of p_T^Z , y_Z^* , and $p+\text{Pb}$ centrality. These corrections take into account the cumulative losses due to trigger, reconstruction, and identification efficiency as well as the kinematic acceptance of the decay leptons. The correction is defined relative to all generated Z bosons within the mass window $66 < m_{\ell\ell} < 116$ GeV. The total efficiency for reconstructing a produced Z boson, including acceptance, is approximately 55% for $Z \rightarrow ee$ and 65% for $Z \rightarrow \mu\mu$. Following the subtraction of background (see Sec 3.5) and application of the correction factor, a corrected yield of Z bosons is obtained in each bin of p_T^Z and y_Z^* . The uncertainty on the correction factor follows from the uncertainty of the data-driven tag-and-probe checks of the MC, primarily due to the relatively low number of tag-and-probe events in the data. The uncertainty associated with the lepton identification efficiency is the dominant uncertainty for both the $Z \rightarrow ee$ and $Z \rightarrow \mu\mu$ analyses. This uncertainty is approximately 10% for $Z \rightarrow ee$ (rising as high as 15% for pairs including a forward-electron), and 1.5% for $Z \rightarrow \mu\mu$. The sizable uncertainty for $Z \rightarrow ee$ is primarily driven by the limited size of the tag-and-probe 2013 $p+\text{Pb}$ dataset. The other uncertainties are typically less than 2% in both channels.

3.5 Yield extraction

To form $Z \rightarrow ee$ candidates, all electrons found in triggered events are paired with each other. When both electrons are at midrapidity ($|\eta| < 2.47$), the unlike-sign charged pairs with an invariant mass satisfying $66 < m_{ee} < 116$ GeV are accepted as signal Z boson candidates. The like-sign pairs in this window are used to estimate the combinatorial background, created primarily by jets. In total, 1647 unlike-sign pairs and 52 like-sign pairs are reconstructed. The like-sign pairs are composed of combinatorial background and $Z \rightarrow ee$ decays in which one of the electrons has misreconstructed charge. The contribution from pairs with misreconstructed charge is estimated, using the MC simulation, to be half of the like-sign pairs, and the remainder is taken as an estimate of the background. Pairs made of one midrapidity electron and one non-triggering forward-electron have a larger contribution from background and so an invariant mass window of $80 < m_{ee} < 100$ GeV is used to select Z boson candidates. To facilitate combination of all $Z \rightarrow ee$ candidates, an acceptance correction is made to account for the smaller mass window. No charge requirement is made for these candidates because the non-triggering electron is outside the

acceptance of the ID and therefore does not have a reconstructed charge. There are 264 such candidates, of which an estimated 5% are background based on a fit of the invariant mass distribution. The fit is performed in the range $60 < m_{ee} < 120$ GeV using a signal shape from the MC simulation, and several background parametrizations assuming exponential or polynomial descriptions of the background. The mass distributions of $Z \rightarrow ee$ candidates are shown in Figure 2(a) and 2(b), along with the reconstructed MC simulation of the same quantity. The estimated background is subtracted from the signal candidates differentially in rapidity, transverse momentum, and centrality.

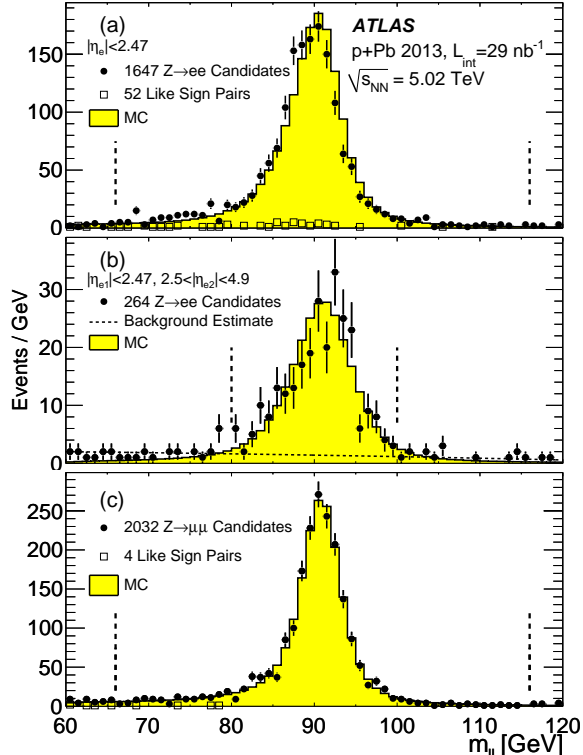


Figure 2: (Color online) The dilepton invariant mass distributions in data and MC simulation. (a) $Z \rightarrow ee$ candidates with both electrons at midrapidity ($|\eta| < 2.47$); (b) candidates in which the non-triggering electron is a forward-electron ($2.5 < |\eta| < 4.9$); (c) $Z \rightarrow \mu\mu$ candidates. The midrapidity $Z \rightarrow ee$ and $Z \rightarrow \mu\mu$ distributions are overlaid with the mass distributions of like-sign lepton pairs. For candidates in which the non-triggering electron is a forward-electron ($2.5 < |\eta| < 4.9$) the background, estimated based on a decomposition of the invariant mass distribution (see text), is shown. In all plots the vertical lines indicate the mass window within which candidates are defined, and the MC simulation is normalized to the data inside this region.

A similar procedure is also followed to select $Z \rightarrow \mu\mu$ candidates with an invariant mass of $66 < m_{\mu\mu} < 116$ GeV. This selection yields 2032 unlike-sign charged candidates and 4 like-sign pairs; their mass distribution is shown in Figure 2(c). The MC simulation describes the data well in both lepton channels. The slight shift of the mass peak visible between the data and the simulation for dielectron events has only a very small effect on the calculation of corrections based on the MC simulation and is incorporated into the systematic uncertainty associated with electron reconstruction.

Based on the like-sign pairs and MC simulation of charge misreconstruction, the uncertainty from the background subtraction is approximately 1% in the $Z \rightarrow ee$ channel for pairs in which both electrons are

at midrapidity; in pairs involving a forward-electron the uncertainty ranges from 5% to 20% based on fits of the invariant mass distribution. The background uncertainty in the $Z \rightarrow \mu\mu$ yield is negligible. The largest source of correlated background in both lepton decay channels is the decay of $Z \rightarrow \tau\tau$ events into dielectron and dimuon pairs. These are simulated and reconstructed just as $Z \rightarrow ee$ and $Z \rightarrow \mu\mu$ are, but are found to have a negligible contribution following the analysis procedures.

3.6 Systematic uncertainties

The dominant source of uncertainty in the $Z \rightarrow ee$ measurement stems from imperfect knowledge of the efficiency of the electron identification requirements. The uncertainty is driven by the limited number of events available for the tag-and-probe analysis which had to rely on 2013 p +Pb collision data because the electron reconstruction performance changed due to detector conditions and occupancy compared to earlier pp collision data. The uncertainty is larger in pairs involving a forward-electron, and the sample has a lower purity than the sample of midrapidity electrons. Other electron uncertainties are significantly smaller and are associated with trigger efficiency, electron reconstruction efficiency and energy resolution, background subtraction (which becomes significant for forward-electrons), and charge misreconstruction. In addition a small uncertainty stems from possible differences between the simulated y_Z^* distribution and the one measured in data. The $Z \rightarrow ee$ systematic uncertainties depend on p_T^Z , y_Z^* , and p +Pb centrality and are summarized in Table 1.

Source	Uncertainty Range [%]
Electron ID	6–14
Electron Reconstruction	1–3
Electron Trigger	1–2
Background	1–3
MC y_Z^* Shape	0–2
Forward-Electron Reconstruction	4–15
Forward-Electron Background	2–10

Table 1: Relative systematic uncertainties, in percent, associated with the measurement of $Z \rightarrow ee$. The uncertainties typically increase at the more forward rapidities. Background includes charge misreconstruction, and electron reconstruction includes resolution. The last two rows refer only to pairs where one of the electrons was reconstructed in the range $3.1 < |\eta| < 4.9$.

The conditions of muon reconstruction in the 2013 p +Pb collision data closely resemble those in pp collisions described in Ref. [24]. The small uncertainties from the more abundant pp data are used in this analysis. An uncertainty of 1%, based on the performance of the muon reconstruction in high-pileup pp collisions, is associated with the scale factors to account for possible differences between the datasets. The uncertainties depend on p_T^Z and y_Z^* . Table 2 summarizes the systematic uncertainties on the $Z \rightarrow \mu\mu$ measurement.

In addition to the Z boson measurement uncertainties, a 2.7% uncertainty is associated with the luminosity calculation. For the centrality-dependent yields that are scaled by $\langle T_{AA} \rangle$ the uncertainties of the Glauber model calculations are taken from Ref. [22]. The correction to centrality due to bias from the presence of a hard scattering, taken from Ref. [30], has uncertainties as shown in Figure 1.

Source	Uncertainty Range [%]
Muon ID & Reconstruction	1.5
Muon Trigger	1–2
Background	<1
p_T Resolution	<1
MC y_Z^* Shape	<1.5

Table 2: Relative systematic uncertainties, in percent, associated with the measurement of $Z \rightarrow \mu\mu$.

3.7 Lepton channel combination

The cross section in each leptonic decay channel is defined for the mass window $66 < m_Z < 116$ GeV, the rapidity ranges $|y_Z^*| < 3.5$ for $Z \rightarrow ee$ and $-3 < y_Z^* < 2$ for $Z \rightarrow \mu\mu$, and the full decay-lepton kinematic phase-space. The $Z \rightarrow ee$ and $Z \rightarrow \mu\mu$ yields, corrected for acceptance and efficiency, are used to calculate the cross section in each channel, and good agreement between the two is observed as is shown for the y_Z^* distributions in Figure 3.

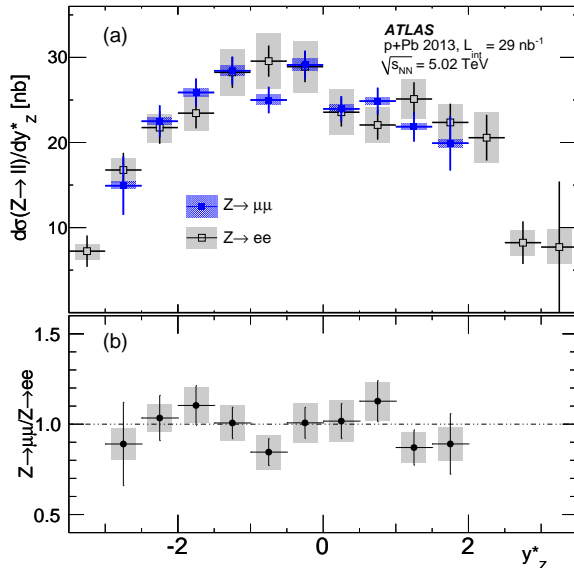


Figure 3: (Color online) (a) Differential Z boson production cross section, $d\sigma/dy_Z^*$, as a function of Z boson rapidity in the center-of-mass frame y_Z^* , for $Z \rightarrow ee$ and $Z \rightarrow \mu\mu$ (upper panel). (b) Their ratio. Bars indicate statistical uncertainty and shaded boxes systematic uncertainty.

The two decay channel results are combined to one set of $Z \rightarrow \ell\ell$ data using the method described in Refs. [35, 36]. The technique uses a χ^2 minimization procedure with a nuisance parameter formalism to combine the data sets coherently. The procedure distinguishes between those systematic uncertainty sources that are uncorrelated bin-to-bin, uncorrelated across data sets, and fully correlated bin-to-bin and across data sets. In this way, combined points are calculated to optimize the overall agreement of the data sets, given the correlation of the uncertainties. This may result in differences in the combined $Z \rightarrow \ell\ell$ data points relative to the $Z \rightarrow ee$ data points in the rapidity regions in which there are no $Z \rightarrow \mu\mu$ data

points. Following this, an integrated cross section for the region $|y_Z^*| < 3.5$ is defined for the combined $Z \rightarrow \ell\ell$ points based on both the $Z \rightarrow ee$ and $Z \rightarrow \mu\mu$ data even though the $Z \rightarrow \mu\mu$ data are limited to $-3 < y_Z^* < 2$. The systematic uncertainties associated with the combined results are fully correlated bin-to-bin in each distribution. They are approximately 3% at midrapidity, and rise to about 10% at forward and backward rapidity.

4 Results

4.1 $Z \rightarrow \ell\ell$ cross section

From the combined $Z \rightarrow ee$ and $Z \rightarrow \mu\mu$ data a total cross section of 139.8 ± 4.8 (statistical) ± 6.2 (systematic) ± 3.8 (luminosity) nb is obtained in the $|y_Z^*| < 3.5$ acceptance. Based on the MC simulation (and the models discussed below) this acceptance covers approximately 99.5% of the total $Z \rightarrow \ell\ell$ cross section. Restricting the results to the smaller rapidity interval of $-3 < y_Z^* < 2$, the cross section is 119.3 ± 2.2 (stat.) ± 3.4 (syst.) ± 3.2 (lumi.) nb. Table 3 lists the integrated cross section in the larger and smaller rapidity ranges as measured for each channel and their combination.

y_Z^*	$[-2, 0]$	$[0, 2]$	$[-3, 2]$	$[-3.5, 3.5]$
$Z \rightarrow \mu\mu$	$54.2 \pm 1.6 \pm 1.3$	$45.3 \pm 2.1 \pm 0.9$	$118.2 \pm 3.3 \pm 2.6$	N/A
$Z \rightarrow ee$	$55.1 \pm 1.8 \pm 5.9$	$46.5 \pm 2.2 \pm 5.0$	$121 \pm 3 \pm 13$	$143 \pm 5 \pm 17$
$Z \rightarrow \ell\ell$	$54.4 \pm 1.3 \pm 1.4$	$45.9 \pm 1.4 \pm 1.4$	$119.3 \pm 2.2 \pm 3.4$	$139.8 \pm 4.8 \pm 6.2$
CT10 (NLO)	47.4 ± 0.9	46.8 ± 0.9	110.8 ± 2.9	132.2 ± 3.3
CT10+EPS09 (NLO)	48.7 ± 1.0	43.5 ± 1.1	108.6 ± 3.1	127.4 ± 3.6
MSTW2008 (NNLO)	$48.3_{-0.9}^{+1.2}$	$47.9_{-0.9}^{+1.2}$	$113.5_{-2.2}^{+2.8}$	$135.2_{-2.7}^{+3.4}$

Table 3: The measured integrated cross section, in nb, for several rapidity ranges, for $Z \rightarrow \mu\mu$, $Z \rightarrow ee$, and the combined $Z \rightarrow \ell\ell$. The first uncertainty listed is statistical and the second systematic. There is an additional 2.7% luminosity uncertainty on each cross section. The cross sections predicted by the models (see text) are also shown. The uncertainties listed with the model calculations are the PDF and scale uncertainties added in quadrature.

The measured cross section may be compared to a p +Pb model prediction composed of a linear sum of the nucleon-nucleon cross sections: $82\sigma(pp \rightarrow Z + X) + 126\sigma(pn \rightarrow Z + X)$, corresponding to the numbers of protons and neutrons in the Pb ion. The value of $\sigma(pn \rightarrow Z + X)$ is 2% higher than that of $\sigma(pp \rightarrow Z + X)$ in all models discussed below. Calculating the baseline nucleon-nucleon cross sections using the CT10 PDF at next-to-leading order (NLO), as in the corresponding MC simulation, the model yields values of 132.2 ± 3.3 nb in the range $|y_Z^*| < 3.5$, and 110.8 ± 2.9 nb for $-3 < y_Z^* < 2$ where the uncertainties are the sums in quadrature of PDF and scale (renormalization and factorization) uncertainties. Using the MSTW2008 PDF, calculated with FEWZ [37] at next-to-next-to-leading order (NNLO), cross sections of $135.2_{-2.7}^{+3.4}$ nb are obtained for $|y_Z^*| < 3.5$ and $113.5_{-2.2}^{+2.8}$ nb for $-3 < y_Z^* < 2$. At NLO the results from MSTW2008 are very close to the CT10 results. In addition to the simple model of the p +Pb Z boson cross section as a linear sum of nucleon-nucleon cross sections, calculations are performed incorporating nuclear corrections of the PDF. Including the EPS09 modifications [38] to the CT10 PDF results in cross sections of 127.4 ± 3.6 nb and 108.6 ± 3.1 nb, respectively.

For a more detailed understanding of Z boson production, the measured cross section as a function of the Z boson rapidity is presented in Figure 4 and compared to model calculations. The data are seen to be

strongly asymmetric about $y_Z^*=0$. The CT10+EPS09 calculations come closest to reproducing the shape of the measured y_Z^* differential cross section. A χ^2 test of compatibility between the data and the model shapes (irrespective of normalization) finds that the CT10+EPS09 shape of the y_Z^* distribution gives a p -value of 0.79. The unmodified CT10 calculation and MSTW2008 calculations have p -values of 0.07 and 0.01, respectively. A Kolmogorov-Smirnov test was also performed and resulted in probabilities of 0.96, 0.09, and 0.07 for CT10+EPS09, CT10, and MSTW2008 model calculations. This is consistent with the preference for the observation of nuclear correction effects as in the χ^2 test.

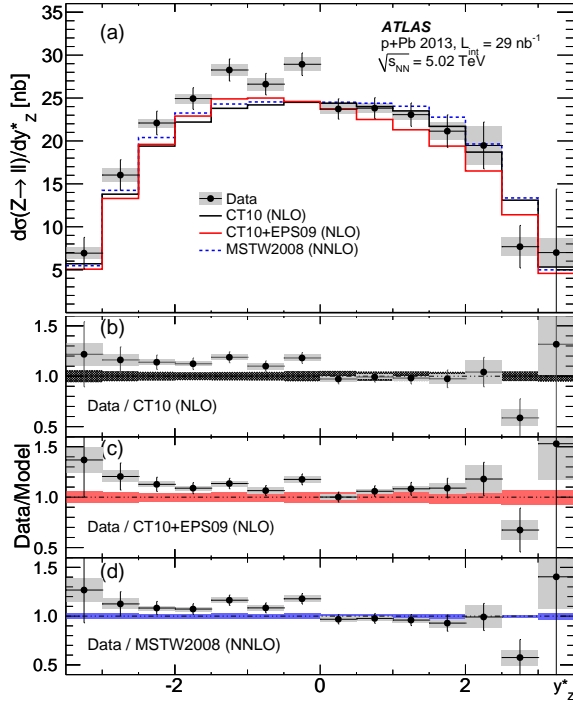


Figure 4: (Color online) (a) The $d\sigma/dy_Z^*$ distribution from $Z \rightarrow \ell\ell$, shown along with several model calculations in the upper panel. The bars indicate statistical uncertainty and the shaded boxes systematic uncertainty on the data; the uncertainties on the model calculations are not shown. (b-d) Ratios of the data to the models. The uncertainties of the model calculations (scale and PDF uncertainties added in quadrature) are shown as bands around unity in each panel. An additional 2.7% luminosity uncertainty on the cross section is not shown.

Nuclear modification of PDFs is fundamentally related to the Bjorken x of the relevant parton. At leading order, x_p in the proton and x_{Pb} in the lead nucleus are related to the reconstructed Z boson kinematics by:

$$x_p = \frac{m_{\ell\ell} e^{y_Z^*}}{\sqrt{s_{NN}}}, \quad x_{Pb} = \frac{m_{\ell\ell} e^{-y_Z^*}}{\sqrt{s_{NN}}}. \quad (1)$$

The resulting x_{Pb} distribution is shown in Figure 5 and compared to model calculations.

Figure 6 shows the p_T^Z distributions for $-3 < y_Z^* < 2$, and separately for $-2 < y_Z^* < 0$ and $0 < y_Z^* < 2$. These are compared to the baseline CT10 model. The p_T^Z dependence is less sensitive to nuclear effects and good agreement between the experimental measurement and the MC simulation shape is observed.

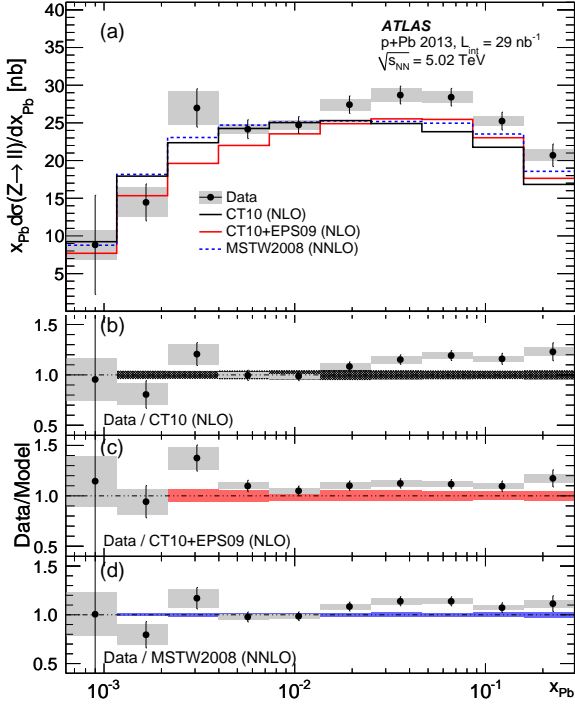


Figure 5: (Color online) (a) The differential cross section of Z boson production multiplied by the Bjorken x of the parton in the lead nucleus, $x_{Pb}d\sigma/dx_{Pb}$, as a function of x_{Pb} using $Z \rightarrow \ell\ell$ events shown along with several model calculations in the upper panel. The bars indicate statistical uncertainty and the shaded boxes systematic uncertainty on the data; the uncertainties on the model calculations are not shown. (b-d) Ratios of the data to the models. The uncertainties of the model calculations are shown as bands around unity in each panel. There is an additional 2.7% luminosity uncertainty on the cross section.

4.2 Centrality-dependent yield

Results are presented for the centrality-dependent Z boson yield. If the rate of Z boson production were consistent with geometric expectations, then the Z boson yield divided by $\langle N_{\text{coll}} \rangle$ should be independent of centrality. To investigate this, the yield of Z bosons per event scaled by $\langle N_{\text{coll}} \rangle$, within $-3 < y_Z^* < 2$, is displayed as a function of $\langle N_{\text{part}} \rangle$ in Figure 7. The yield is independent of centrality defined using the standard Glauber model. Using the GGCF centrality models increases $\langle N_{\text{coll}} \rangle$ in central events and reduces it in peripheral events, consequently the yield divided by $\langle N_{\text{coll}} \rangle$ is reduced in central events and increased in peripheral events. Figure 7 also shows the yield without the application of the centrality bias corrections discussed in Sec. 3.3.

The ATLAS Collaboration has previously measured the inclusive charged-hadron multiplicity in $p+\text{Pb}$ collisions as a function of centrality [22], and the centrality dependence of that quantity is similar to that observed in the present measurement. In order to quantify the similarity, the ratio $(dN_Z/dy_Z^*)/(dN_{\text{ch}}/d\eta)$ is plotted vs $\langle N_{\text{part}} \rangle$ in Figure 8. The charged-particle yield is expected to scale with $\langle N_{\text{part}} \rangle$ and the Z boson yield with $\langle N_{\text{coll}} \rangle = \langle N_{\text{part}} \rangle - 1$, and so the ratio is fit to a function with the form $a \cdot (\langle N_{\text{part}} \rangle - 1)/\langle N_{\text{part}} \rangle$. This function describes the data well for the GGCF cases, and less so for the standard Glauber model.

To further investigate the behavior observed in the rapidity differential cross section, the y_Z^* dependence of the Z boson yield in different centrality bins is also measured, as shown in Figure 9. The differences

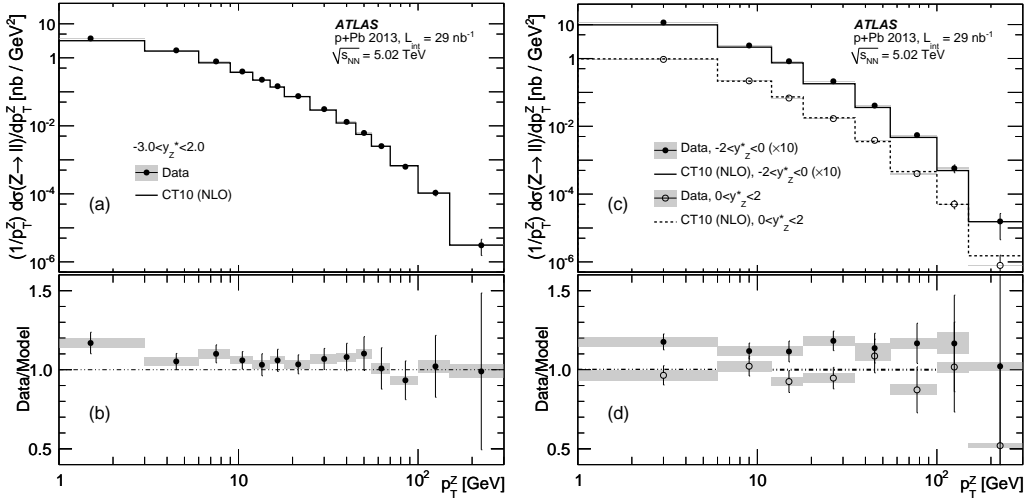


Figure 6: (Color online) (a, c) The distributions of the differential cross section of Z boson production as a function of the transverse momentum of the Z , p_T^Z , shown along with the CT10 model calculation. (b, d) Ratio of the data to the model. (a,b) for $-3 < y_Z^* < 2$; (c,d) for $-2 < y_Z^* < 0$ and $0 < y_Z^* < 2$. The bars indicate statistical uncertainty and the shaded boxes systematic uncertainty. The leftmost bin represents the range 0–3 GeV. An additional 2.7% luminosity uncertainty of the cross section is not shown.

between data and the model are larger in central collisions. The $\langle N_{\text{coll}} \rangle$ -scaled ratio of central to peripheral data, R_{CP} , defined as

$$R_{\text{CP}}(y_Z^*) = \frac{\langle N_{\text{coll}} \rangle^{\text{peripheral}}}{\langle N_{\text{coll}} \rangle^{\text{central}}} \times \frac{dN_Z^{\text{central}}/dy_Z^*}{dN_Z^{\text{peripheral}}/dy_Z^*} \quad (2)$$

is used to observe changes in the rapidity distribution for different centrality bins in a model-independent way and is shown in Figure 9. Events with 40–90% centrality define the peripheral event selection, and two central selections, 0–10% and 10–40%, are compared with it. A linear fit of the $R_{\text{CP}}(y_Z^*)$ for 0–10% centrality, results in a slope of -0.11 ± 0.04 , which suggests that the y_Z^* distribution may be different in the most central events compared to peripheral events. For 10–40% centrality, the slope is -0.05 ± 0.03 .

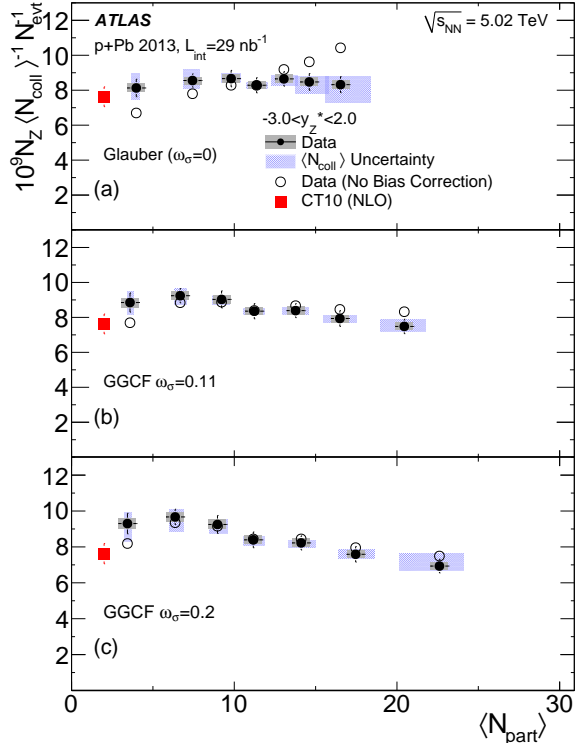


Figure 7: (Color online) The yield of Z bosons per event scaled by the mean number of nucleon-nucleon collisions $\langle N_{\text{coll}} \rangle$ as a function of the mean number of participating nucleons $\langle N_{\text{part}} \rangle$. Each panel uses a different Glauber model configuration in calculating $\langle N_{\text{part}} \rangle$ (and $\langle N_{\text{coll}} \rangle$). (a) Standard Glauber model with no Glauber-Gribov color fluctuations; (b) GGCF with $\omega_\sigma = 0.11$; (c) GGCF with $\omega_\sigma = 0.2$. The data are compared to the CT10 model prediction plotted at $\langle N_{\text{part}} \rangle = 2$. The bars indicate statistical uncertainty and the shaded boxes systematic uncertainty. The systematic uncertainties are correlated bin-by-bin. The $\langle N_{\text{coll}} \rangle$ uncertainty plotted does not include the bin-by-bin fully correlated uncertainty stemming from the uncertainty on $\sigma(N + N \rightarrow X)$, which is instead included in the CT10 prediction uncertainty. As a reference, the data are plotted as they would be with no centrality bias correction in the open points.

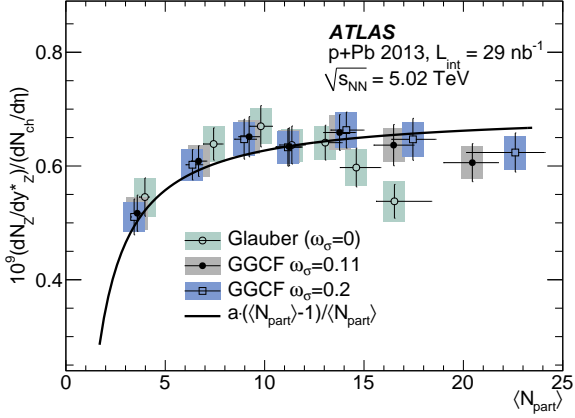


Figure 8: (Color online) The ratio of the Z boson multiplicity to the inclusive charged particle multiplicity, $(dN_Z/dy_Z^*)/(dN_{ch}/d\eta)$, as a function of $\langle N_{part} \rangle$. A function of the form $a \cdot (\langle N_{part} \rangle - 1)/\langle N_{part} \rangle$ is also shown. The normalization a is set based on the GGCF with $\omega_\sigma = 0.11$ points. Statistical uncertainties are plotted as bars and systematic uncertainties as shaded boxes.

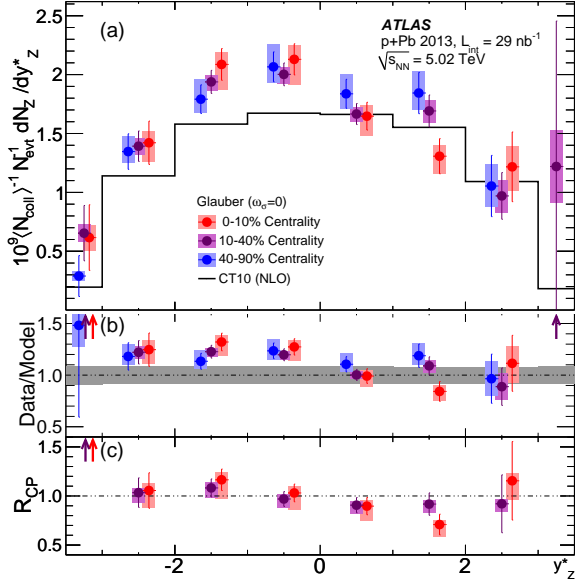


Figure 9: (Color online) (a) The rapidity differential Z boson yields, scaled by $\langle N_{coll} \rangle$, for three centrality ranges compared with the CT10 model calculation. The bars indicate statistical uncertainty and the shaded boxes systematic uncertainty. The $\langle N_{coll} \rangle$ is defined with the standard Glauber model ($\omega_\sigma=0$). The scale uncertainty stemming from the centrality calculation for each bin is included in the systematic uncertainty. The uncertainty associated with the model is not plotted. (b) The ratios of the data to the model. The uncertainty of the model added in quadrature with the scale uncertainty due to uncertainty in the inclusive NN cross section is shown as a band around unity. (c) R_{CP} (see text for details). The 0–10% and 40–90% centrality points are offset for visual clarity. The arrows in the lower panels indicate values outside the plotted axes.

5 Summary

The Z boson production cross section has been measured in $p+\text{Pb}$ collisions at $\sqrt{s_{\text{NN}}} = 5.02 \text{ TeV}$ with the ATLAS detector at the LHC, using $Z \rightarrow ee$ ($Z \rightarrow \mu\mu$) decays in a 29.4 nb^{-1} (28.1 nb^{-1}) data sample. It is found to be slightly higher than predictions based on perturbative QCD calculations. Disregarding the difference in overall normalization, the shapes of the y_Z^* and x_{Pb} -dependent cross sections are somewhat better described by models that include nuclear modification of the lead nucleus PDF compared to those that do not, although models without nuclear modification are not excluded. Following the application of a centrality bias correction, the centrality-dependent yield is found to scale with $\langle N_{\text{coll}} \rangle$. In addition, the centrality dependence of the y_Z^* distribution was studied, and the asymmetry in y_Z^* was found to be slightly larger in more central events. Integrated over y_Z^* , the centrality dependence appears to be consistent with binary scaling and is similar to the production of inclusive charged particles.

Acknowledgments

We thank CERN for the very successful operation of the LHC, as well as the support staff from our institutions without whom ATLAS could not be operated efficiently.

We acknowledge the support of ANPCyT, Argentina; YerPhI, Armenia; ARC, Australia; BMWFW and FWF, Austria; ANAS, Azerbaijan; SSTC, Belarus; CNPq and FAPESP, Brazil; NSERC, NRC and CFI, Canada; CERN; CONICYT, Chile; CAS, MOST and NSFC, China; COLCIENCIAS, Colombia; MSMT CR, MPO CR and VSC CR, Czech Republic; DNRF, DNSRC and Lundbeck Foundation, Denmark; EPLANET, ERC and NSRF, European Union; IN2P3-CNRS, CEA-DSM/IRFU, France; GNSF, Georgia; BMBF, DFG, HGF, MPG and AvH Foundation, Germany; GSRT and NSRF, Greece; RGC, Hong Kong SAR, China; ISF, MINERVA, GIF, I-CORE and Benoziyo Center, Israel; INFN, Italy; MEXT and JSPS, Japan; CNRST, Morocco; FOM and NWO, Netherlands; BRF and RCN, Norway; MNiSW and NCN, Poland; GRICES and FCT, Portugal; MNE/IFA, Romania; MES of Russia and NRC KI, Russian Federation; JINR; MSTD, Serbia; MSSR, Slovakia; ARRS and MIZŠ, Slovenia; DST/NRF, South Africa; MINECO, Spain; SRC and Wallenberg Foundation, Sweden; SER, SNSF and Cantons of Bern and Geneva, Switzerland; NSC, Taiwan; TAEK, Turkey; STFC, the Royal Society and Leverhulme Trust, United Kingdom; DOE and NSF, United States of America.

The crucial computing support from all WLCG partners is acknowledged gratefully, in particular from CERN and the ATLAS Tier-1 facilities at TRIUMF (Canada), NDGF (Denmark, Norway, Sweden), CC-IN2P3 (France), KIT/GridKA (Germany), INFN-CNAF (Italy), NL-T1 (Netherlands), PIC (Spain), ASGC (Taiwan), RAL (UK) and BNL (USA) and in the Tier-2 facilities worldwide.

References

- [1] CMS Collaboration, [Phys. Lett. **B710** \(2012\) 256–277](#).
- [2] CMS Collaboration, [Phys. Lett. **B715** \(2012\) 66–87](#).
- [3] ATLAS Collaboration, [Eur. Phys. J. **C75** no. 1, \(2015\) 23](#).
- [4] ATLAS Collaboration, [Phys. Rev. Lett. **110** no. 2, \(2013\) 022301](#).

- [5] CMS Collaboration, [JHEP **1503** \(2015\) 022](#).
- [6] T. Sjöstrand, S. Mrenna, and P. Z. Skands, [Comput. Phys. Commun. **178** \(2008\) 852–867](#).
- [7] H. Paukkunen, [PoS **DIS2014** \(2014\) 053](#), [arXiv:1408.4657 \[hep-ph\]](#).
- [8] ALICE Collaboration, B. Abelev et al., [Phys. Lett. **B719** \(2013\) 29–41](#).
- [9] CMS Collaboration, [Phys. Lett. **B718** \(2013\) 795–814](#).
- [10] ATLAS Collaboration, [Phys. Rev. Lett. **110** no. 18, \(2013\) 182302](#).
- [11] ALICE Collaboration, B. Abelev et al., [Phys. Lett. **B726** \(2013\) 164–177](#).
- [12] CMS Collaboration, [Phys. Lett. **B724** \(2013\) 213–240](#).
- [13] ATLAS Collaboration, [Phys. Lett. **B725** \(2013\) 60–78](#).
- [14] ATLAS Collaboration, [Phys. Rev. **C90** no. 4, \(2014\) 044906](#).
- [15] ATLAS Collaboration, [Phys. Lett. **B748** \(2015\) 392–413](#).
- [16] CMS Collaboration, [Eur. Phys. J. **C74** no. 7, \(2014\) 2951](#).
- [17] CMS Collaboration, [Phys. Lett. **B750** \(2015\) 565–586](#).
- [18] LHCb Collaboration, R. Aaij et al., [JHEP **1409** \(2014\) 030](#).
- [19] ATLAS Collaboration, [Eur. Phys. J. **C73** no. 8, \(2013\) 2518](#).
- [20] ATLAS Collaboration, [Eur. Phys. J. **C72** \(2012\) 1849](#).
- [21] ATLAS Collaboration, [Eur. Phys. J. **C73** \(2013\) 1–39](#).
- [22] ATLAS Collaboration, [arXiv:1508.00848 \[hep-ex\]](#).
- [23] ATLAS Collaboration, [Eur. Phys. J. **C74** no. 7, \(2014\) 2941](#).
- [24] ATLAS Collaboration, [Eur. Phys. J. **C74** no. 11, \(2014\) 3130](#).
- [25] M. L. Miller, K. Reygers, S. J. Sanders, and P. Steinberg, [Ann.Rev.Nucl.Part.Sci. **57** \(2007\) 205–243](#).
- [26] V. Guzey and M. Strikman, [Phys. Lett. **B633** \(2006\) 245–252](#).
- [27] M. Alvioli and M. Strikman, [Phys. Lett. **B722** \(2013\) 347–354](#).
- [28] PHENIX Collaboration, A. Adare et al., [Phys. Rev. **C90** no. 3, \(2014\) 034902](#).
- [29] ALICE Collaboration, J. Adam et al., [Phys. Rev. **C91** no. 6, \(2015\) 064905](#).
- [30] D. V. Perepelitsa and P. A. Steinberg, [arXiv:1412.0976 \[nucl-ex\]](#).
- [31] S. Alioli, P. Nason, C. Oleari, and E. Re, [JHEP **0807** \(2008\) 060](#).
- [32] H.-L. Lai, M. Guzzi, J. Huston, Z. Li, P. M. Nadolsky, J. Pumplin, and C.-P. Yuan, [Phys. Rev. **D82** \(2010\) 074024](#).
- [33] GEANT4 Collaboration, S. Agostinelli et al., [Nucl. Instrum. Meth. **A506** \(2003\) 250–303](#).
- [34] ATLAS Collaboration, [Eur. Phys. J. **C70** \(2010\) 823–874](#).

- [35] A. Glazov, [AIP Conference Proceedings](#) **792** (2005) 237–240.
- [36] H1 Collaboration, F. Aaron et al., [Eur. Phys. J. C](#) **63** (2009) 625–678.
- [37] R. Gavin, Y. Li, F. Petriello, and S. Quackenbush, [Comput. Phys. Commun.](#) **182** (2011) 2388–2403.
- [38] H. Paukkunen and C. A. Salgado, [JHEP](#) **1103** (2011) 071.

The ATLAS Collaboration

G. Aad⁸⁵, B. Abbott¹¹³, J. Abdallah¹⁵¹, O. Abdinov¹¹, R. Aben¹⁰⁷, M. Abolins⁹⁰, O.S. AbouZeid¹⁵⁸, H. Abramowicz¹⁵³, H. Abreu¹⁵², R. Abreu¹¹⁶, Y. Abulaiti^{146a,146b}, B.S. Acharya^{164a,164b,^a}, L. Adamczyk^{38a}, D.L. Adams²⁵, J. Adelman¹⁰⁸, S. Adomeit¹⁰⁰, T. Adye¹³¹, A.A. Affolder⁷⁴, T. Agatonovic-Jovin¹³, J. Agricola⁵⁴, J.A. Aguilar-Saavedra^{126a,126f}, S.P. Ahlen²², F. Ahmadov^{65,b}, G. Aielli^{133a,133b}, H. Akerstedt^{146a,146b}, T.P.A. Åkesson⁸¹, A.V. Akimov⁹⁶, G.L. Alberghi^{20a,20b}, J. Albert¹⁶⁹, S. Albrand⁵⁵, M.J. Alconada Verzini⁷¹, M. Aleksi³⁰, I.N. Aleksandrov⁶⁵, C. Alexa^{26a}, G. Alexander¹⁵³, T. Alexopoulos¹⁰, M. Alhroob¹¹³, G. Alimonti^{91a}, L. Alio⁸⁵, J. Alison³¹, S.P. Alkire³⁵, B.M.M. Allbrooke¹⁴⁹, P.P. Allport⁷⁴, A. Aloisio^{104a,104b}, A. Alonso³⁶, F. Alonso⁷¹, C. Alpigiani⁷⁶, A. Altheimer³⁵, B. Alvarez Gonzalez³⁰, D. Álvarez Piqueras¹⁶⁷, M.G. Alvaggi^{104a,104b}, B.T. Amadio¹⁵, K. Amako⁶⁶, Y. Amaral Coutinho^{24a}, C. Amelung²³, D. Amidei⁸⁹, S.P. Amor Dos Santos^{126a,126c}, A. Amorim^{126a,126b}, S. Amoroso⁴⁸, N. Amram¹⁵³, G. Amundsen²³, C. Anastopoulos¹³⁹, L.S. Ancu⁴⁹, N. Andari¹⁰⁸, T. Andeen³⁵, C.F. Anders^{58b}, G. Anders³⁰, J.K. Anders⁷⁴, K.J. Anderson³¹, A. Andreazza^{91a,91b}, V. Andrei^{58a}, S. Angelidakis⁹, I. Angelozzi¹⁰⁷, P. Anger⁴⁴, A. Angerami³⁵, F. Anghinolfi³⁰, A.V. Anisenkov^{109,c}, N. Anjos¹², A. Annovi^{124a,124b}, M. Antonelli⁴⁷, A. Antonov⁹⁸, J. Antos^{144b}, F. Anulli^{132a}, M. Aoki⁶⁶, L. Aperio Bella¹⁸, G. Arabidze⁹⁰, Y. Arai⁶⁶, J.P. Araque^{126a}, A.T.H. Arce⁴⁵, F.A. Arduh⁷¹, J-F. Arguin⁹⁵, S. Argyropoulos⁴², M. Arik^{19a}, A.J. Armbruster³⁰, O. Arnaez³⁰, V. Arnal⁸², H. Arnold⁴⁸, M. Arratia²⁸, O. Arslan²¹, A. Artamonov⁹⁷, G. Artoni²³, S. Asai¹⁵⁵, N. Asbah⁴², A. Ashkenazi¹⁵³, B. Åsman^{146a,146b}, L. Asquith¹⁴⁹, K. Assamagan²⁵, R. Astalos^{144a}, M. Atkinson¹⁶⁵, N.B. Atlay¹⁴¹, K. Augsten¹²⁸, M. Aurousseau^{145b}, G. Avolio³⁰, B. Axen¹⁵, M.K. Ayoub¹¹⁷, G. Azuelos^{95,d}, M.A. Baak³⁰, A.E. Baas^{58a}, M.J. Baca¹⁸, C. Bacci^{134a,134b}, H. Bachacou¹³⁶, K. Bachas¹⁵⁴, M. Backes³⁰, M. Backhaus³⁰, P. Bagiacchi^{132a,132b}, P. Bagnaia^{132a,132b}, Y. Bai^{33a}, T. Bain³⁵, J.T. Baines¹³¹, O.K. Baker¹⁷⁶, E.M. Baldin^{109,c}, P. Balek¹²⁹, T. Balestri¹⁴⁸, F. Balli⁸⁴, E. Banas³⁹, Sw. Banerjee¹⁷³, A.A.E. Bannoura¹⁷⁵, H.S. Bansil¹⁸, L. Barak³⁰, E.L. Barberio⁸⁸, D. Barberis^{50a,50b}, M. Barbero⁸⁵, T. Barillari¹⁰¹, M. Barisonzi^{164a,164b}, T. Barklow¹⁴³, N. Barlow²⁸, S.L. Barnes⁸⁴, B.M. Barnett¹³¹, R.M. Barnett¹⁵, Z. Barnovska⁵, A. Baroncelli^{134a}, G. Barone²³, A.J. Barr¹²⁰, F. Barreiro⁸², J. Barreiro Guimarães da Costa⁵⁷, R. Bartoldus¹⁴³, A.E. Barton⁷², P. Bartos^{144a}, A. Basalaev¹²³, A. Bassalat¹¹⁷, A. Basye¹⁶⁵, R.L. Bates⁵³, S.J. Batista¹⁵⁸, J.R. Batley²⁸, M. Battaglia¹³⁷, M. Bauce^{132a,132b}, F. Bauer¹³⁶, H.S. Bawa^{143,e}, J.B. Beacham¹¹¹, M.D. Beattie⁷², T. Beau⁸⁰, P.H. Beauchemin¹⁶¹, R. Beccherle^{124a,124b}, P. Bechtle²¹, H.P. Beck^{17,f}, K. Becker¹²⁰, M. Becker⁸³, S. Becker¹⁰⁰, M. Beckingham¹⁷⁰, C. Becot¹¹⁷, A.J. Beddall^{19b}, A. Beddall^{19b}, V.A. Bednyakov⁶⁵, C.P. Bee¹⁴⁸, L.J. Beemster¹⁰⁷, T.A. Beermann¹⁷⁵, M. Begel²⁵, J.K. Behr¹²⁰, C. Belanger-Champagne⁸⁷, W.H. Bell⁴⁹, G. Bella¹⁵³, L. Bellagamba^{20a}, A. Bellerive²⁹, M. Bellomo⁸⁶, K. Belotskiy⁹⁸, O. Beltramello³⁰, O. Benary¹⁵³, D. Benchekroun^{135a}, M. Bender¹⁰⁰, K. Bendtz^{146a,146b}, N. Benekos¹⁰, Y. Benhammou¹⁵³, E. Benhar Noccioli⁴⁹, J.A. Benitez Garcia^{159b}, D.P. Benjamin⁴⁵, J.R. Bensinger²³, S. Bentvelsen¹⁰⁷, L. Beresford¹²⁰, M. Beretta⁴⁷, D. Berge¹⁰⁷, E. Bergeaas Kuutmann¹⁶⁶, N. Berger⁵, F. Berghaus¹⁶⁹, J. Beringer¹⁵, C. Bernard²², N.R. Bernard⁸⁶, C. Bernius¹¹⁰, F.U. Bernlochner²¹, T. Berry⁷⁷, P. Berta¹²⁹, C. Bertella⁸³, G. Bertoli^{146a,146b}, F. Bertolucci^{124a,124b}, C. Bertsche¹¹³, D. Bertsche¹¹³, M.I. Besana^{91a}, G.J. Besjes³⁶, O. Bessidskaia Bylund^{146a,146b}, M. Bessner⁴², N. Besson¹³⁶, C. Betancourt⁴⁸, S. Bethke¹⁰¹, A.J. Bevan⁷⁶, W. Bhimji¹⁵, R.M. Bianchi¹²⁵, L. Bianchini²³, M. Bianco³⁰, O. Biebel¹⁰⁰, D. Biedermann¹⁶, S.P. Bieniek⁷⁸, M. Biglietti^{134a}, J. Bilbao De Mendizabal⁴⁹, H. Bilokon⁴⁷, M. Bind⁵⁴, S. Binet¹¹⁷, A. Bingul^{19b}, C. Bini^{132a,132b}, S. Biondi^{20a,20b}, C.W. Black¹⁵⁰, J.E. Black¹⁴³, K.M. Black²², D. Blackburn¹³⁸, R.E. Blair⁶, J.-B. Blanchard¹³⁶, J.E. Blanco⁷⁷, T. Blazek^{144a}, I. Bloch⁴², C. Blocker²³, W. Blum^{83,*}, U. Blumenschein⁵⁴, G.J. Bobbink¹⁰⁷, V.S. Bobrovnikov^{109,c}, S.S. Bocchetta⁸¹, A. Bocci⁴⁵,

C. Bock¹⁰⁰, M. Boehler⁴⁸, J.A. Bogaerts³⁰, D. Bogavac¹³, A.G. Bogdanchikov¹⁰⁹, C. Bohm^{146a},
 V. Boisvert⁷⁷, T. Bold^{38a}, V. Boldea^{26a}, A.S. Boldyrev⁹⁹, M. Bomben⁸⁰, M. Bona⁷⁶, M. Boonekamp¹³⁶,
 A. Borisov¹³⁰, G. Borissov⁷², S. Borroni⁴², J. Bortfeldt¹⁰⁰, V. Bortolotto^{60a,60b,60c}, K. Bos¹⁰⁷,
 D. Boscherini^{20a}, M. Bosman¹², J. Boudreau¹²⁵, J. Bouffard², E.V. Bouhova-Thacker⁷²,
 D. Boumediene³⁴, C. Bourdarios¹¹⁷, N. Bousson¹¹⁴, A. Boveia³⁰, J. Boyd³⁰, I.R. Boyko⁶⁵, I. Bozic¹³,
 J. Bracinik¹⁸, A. Brandt⁸, G. Brandt⁵⁴, O. Brandt^{58a}, U. Bratzler¹⁵⁶, B. Brau⁸⁶, J.E. Brau¹¹⁶,
 H.M. Braun^{175,*}, S.F. Brazzale^{164a,164c}, W.D. Breaden Madden⁵³, K. Brendlinger¹²², A.J. Brennan⁸⁸,
 L. Brenner¹⁰⁷, R. Brenner¹⁶⁶, S. Bressler¹⁷², K. Bristow^{145c}, T.M. Bristow⁴⁶, D. Britton⁵³, D. Britzger⁴²,
 F.M. Brochu²⁸, I. Brock²¹, R. Brock⁹⁰, J. Bronner¹⁰¹, G. Brooijmans³⁵, T. Brooks⁷⁷, W.K. Brooks^{32b},
 J. Brosamer¹⁵, E. Brost¹¹⁶, J. Brown⁵⁵, P.A. Bruckman de Renstrom³⁹, D. Bruncko^{144b}, R. Bruneliere⁴⁸,
 A. Bruni^{20a}, G. Bruni^{20a}, M. Bruschi^{20a}, N. Bruscino²¹, L. Bryngemark⁸¹, T. Buanes¹⁴, Q. Buat¹⁴²,
 P. Buchholz¹⁴¹, A.G. Buckley⁵³, S.I. Buda^{26a}, I.A. Budagov⁶⁵, F. Buehrer⁴⁸, L. Bugge¹¹⁹,
 M.K. Bugge¹¹⁹, O. Bulekov⁹⁸, D. Bullock⁸, H. Burckhart³⁰, S. Burdin⁷⁴, B. Burghgrave¹⁰⁸, S. Burke¹³¹,
 I. Burmeister⁴³, E. Busato³⁴, D. Büscher⁴⁸, V. Büscher⁸³, P. Bussey⁵³, J.M. Butler²², A.I. Butt³,
 C.M. Buttar⁵³, J.M. Butterworth⁷⁸, P. Butti¹⁰⁷, W. Buttinger²⁵, A. Buzatu⁵³, A.R. Buzykaev^{109,c},
 S. Cabrera Urbán¹⁶⁷, D. Caforio¹²⁸, V.M. Cairo^{37a,37b}, O. Cakir^{4a}, N. Calace⁴⁹, P. Calafiura¹⁵,
 A. Calandri¹³⁶, G. Calderini⁸⁰, P. Calfayan¹⁰⁰, L.P. Caloba^{24a}, D. Calvet³⁴, S. Calvet³⁴,
 R. Camacho Toro³¹, S. Camarda⁴², P. Camarri^{133a,133b}, D. Cameron¹¹⁹, R. Caminal Armadans¹⁶⁵,
 S. Campana³⁰, M. Campanelli⁷⁸, A. Campoverde¹⁴⁸, V. Canale^{104a,104b}, A. Canepa^{159a}, M. Cano Bret^{33e},
 J. Cantero⁸², R. Cantrill^{126a}, T. Cao⁴⁰, M.D.M. Capeans Garrido³⁰, I. Caprini^{26a}, M. Caprini^{26a},
 M. Capua^{37a,37b}, R. Caputo⁸³, R. Cardarelli^{133a}, F. Cardillo⁴⁸, T. Carli³⁰, G. Carlino^{104a},
 L. Carminati^{91a,91b}, S. Caron¹⁰⁶, E. Carquin^{32a}, G.D. Carrillo-Montoya⁸, J.R. Carter²⁸,
 J. Carvalho^{126a,126c}, D. Casadei⁷⁸, M.P. Casado¹², M. Casolino¹², E. Castaneda-Miranda^{145b},
 A. Castelli¹⁰⁷, V. Castillo Gimenez¹⁶⁷, N.F. Castro^{126a,g}, P. Catastini⁵⁷, A. Catinaccio³⁰, J.R. Catmore¹¹⁹,
 A. Cattai³⁰, J. Caudron⁸³, V. Cavaliere¹⁶⁵, D. Cavalli^{91a}, M. Cavalli-Sforza¹², V. Cavasinni^{124a,124b},
 F. Ceradini^{134a,134b}, B.C. Cerio⁴⁵, K. Cerny¹²⁹, A.S. Cerqueira^{24b}, A. Cerri¹⁴⁹, L. Cerrito⁷⁶, F. Cerutti¹⁵,
 M. Cerv³⁰, A. Cervelli¹⁷, S.A. Cetin^{19c}, A. Chafaq^{135a}, D. Chakraborty¹⁰⁸, I. Chalupkova¹²⁹,
 P. Chang¹⁶⁵, J.D. Chapman²⁸, D.G. Charlton¹⁸, C.C. Chau¹⁵⁸, C.A. Chavez Barajas¹⁴⁹, S. Cheatham¹⁵²,
 A. Chegwidden⁹⁰, S. Chekanov⁶, S.V. Chekulaev^{159a}, G.A. Chelkov^{65,h}, M.A. Chelstowska⁸⁹,
 C. Chen⁶⁴, H. Chen²⁵, K. Chen¹⁴⁸, L. Chen^{33d,i}, S. Chen^{33c}, X. Chen^{33f}, Y. Chen⁶⁷, H.C. Cheng⁸⁹,
 Y. Cheng³¹, A. Cheplakov⁶⁵, E. Cheremushkina¹³⁰, R. Cherkaoui El Moursli^{135e}, V. Chernyatin^{25,*},
 E. Cheu⁷, L. Chevalier¹³⁶, V. Chiarella⁴⁷, G. Chiarelli^{124a,124b}, J.T. Childers⁶, G. Chiodini^{73a},
 A.S. Chisholm¹⁸, R.T. Chislett⁷⁸, A. Chitan^{26a}, M.V. Chizhov⁶⁵, K. Choi⁶¹, S. Chouridou⁹,
 B.K.B. Chow¹⁰⁰, V. Christodoulou⁷⁸, D. Chromek-Burckhart³⁰, J. Chudoba¹²⁷, A.J. Chuinard⁸⁷,
 J.J. Chwastowski³⁹, L. Chytka¹¹⁵, G. Ciapetti^{132a,132b}, A.K. Ciftci^{4a}, D. Cinca⁵³, V. Cindro⁷⁵,
 I.A. Cioara²¹, A. Ciocio¹⁵, Z.H. Citron¹⁷², M. Ciubancan^{26a}, A. Clark⁴⁹, B.L. Clark⁵⁷, P.J. Clark⁴⁶,
 R.N. Clarke¹⁵, W. Cleland¹²⁵, C. Clement^{146a,146b}, Y. Coadou⁸⁵, M. Cobal^{164a,164c}, A. Coccaro¹³⁸,
 J. Cochran⁶⁴, L. Coffey²³, J.G. Cogan¹⁴³, L. Colasurdo¹⁰⁶, B. Cole³⁵, S. Cole¹⁰⁸, A.P. Colijn¹⁰⁷,
 J. Collot⁵⁵, T. Colombo^{58c}, G. Compostella¹⁰¹, P. Conde Muiño^{126a,126b}, E. Coniavitis⁴⁸,
 S.H. Connell^{145b}, I.A. Connelly⁷⁷, S.M. Consonni^{91a,91b}, V. Consorti⁴⁸, S. Constantinescu^{26a},
 C. Conta^{121a,121b}, G. Conti³⁰, F. Conventi^{104a,j}, M. Cooke¹⁵, B.D. Cooper⁷⁸, A.M. Cooper-Sarkar¹²⁰,
 T. Cornelissen¹⁷⁵, M. Corradi^{20a}, F. Corriveau^{87,k}, A. Corso-Radu¹⁶³, A. Cortes-Gonzalez¹²,
 G. Cortiana¹⁰¹, G. Costa^{91a}, M.J. Costa¹⁶⁷, D. Costanzo¹³⁹, D. Côté⁸, G. Cottin²⁸, G. Cowan⁷⁷,
 B.E. Cox⁸⁴, K. Cranmer¹¹⁰, G. Cree²⁹, S. Crépé-Renaudin⁵⁵, F. Crescioli⁸⁰, W.A. Cribbs^{146a,146b},
 M. Crispin Ortuzar¹²⁰, M. Cristinziani²¹, V. Croft¹⁰⁶, G. Crosetti^{37a,37b}, T. Cuhadar Donszelmann¹³⁹,
 J. Cummings¹⁷⁶, M. Curatolo⁴⁷, C. Cuthbert¹⁵⁰, H. Czirr¹⁴¹, P. Czodrowski³, S. D'Auria⁵³,
 M. D'Onofrio⁷⁴, M.J. Da Cunha Sargedas De Sousa^{126a,126b}, C. Da Via⁸⁴, W. Dabrowski^{38a},

A. Dafinca¹²⁰, T. Dai⁸⁹, O. Dale¹⁴, F. Dallaire⁹⁵, C. Dallapiccola⁸⁶, M. Dam³⁶, J.R. Dandoy³¹, N.P. Dang⁴⁸, A.C. Daniells¹⁸, M. Danninger¹⁶⁸, M. Dano Hoffmann¹³⁶, V. Dao⁴⁸, G. Darbo^{50a}, S. Darmora⁸, J. Dassoulas³, A. Dattagupta⁶¹, W. Davey²¹, C. David¹⁶⁹, T. Davidek¹²⁹, E. Davies^{120,l}, M. Davies¹⁵³, P. Davison⁷⁸, Y. Davygora^{58a}, E. Dawe⁸⁸, I. Dawson¹³⁹, R.K. Daya-Ishmukhametova⁸⁶, K. De⁸, R. de Asmundis^{104a}, A. De Benedetti¹¹³, S. De Castro^{20a,20b}, S. De Cecco⁸⁰, N. De Groot¹⁰⁶, P. de Jong¹⁰⁷, H. De la Torre⁸², F. De Lorenzi⁶⁴, L. De Nooij¹⁰⁷, D. De Pedis^{132a}, A. De Salvo^{132a}, U. De Sanctis¹⁴⁹, A. De Santo¹⁴⁹, J.B. De Vivie De Regie¹¹⁷, W.J. Dearnaley⁷², R. Debbe²⁵, C. Debenedetti¹³⁷, D.V. Dedovich⁶⁵, I. Deigaard¹⁰⁷, J. Del Peso⁸², T. Del Prete^{124a,124b}, D. Delgove¹¹⁷, F. Deliot¹³⁶, C.M. Delitzsch⁴⁹, M. Deliyergiyev⁷⁵, A. Dell'Acqua³⁰, L. Dell'Asta²², M. Dell'Orso^{124a,124b}, M. Della Pietra^{104a,j}, D. della Volpe⁴⁹, M. Delmastro⁵, P.A. Delsart⁵⁵, C. Deluca¹⁰⁷, D.A. DeMarco¹⁵⁸, S. Demers¹⁷⁶, M. Demichev⁶⁵, A. Demilly⁸⁰, S.P. Denisov¹³⁰, D. Derendarz³⁹, J.E. Derkaoui^{135d}, F. Derue⁸⁰, P. Dervan⁷⁴, K. Desch²¹, C. Deterre⁴², P.O. Deviveiros³⁰, A. Dewhurst¹³¹, S. Dhaliwal²³, A. Di Ciaccio^{133a,133b}, L. Di Ciaccio⁵, A. Di Domenico^{132a,132b}, C. Di Donato^{104a,104b}, A. Di Girolamo³⁰, B. Di Girolamo³⁰, A. Di Mattia¹⁵², B. Di Micco^{134a,134b}, R. Di Nardo⁴⁷, A. Di Simone⁴⁸, R. Di Sipio¹⁵⁸, D. Di Valentino²⁹, C. Diaconu⁸⁵, M. Diamond¹⁵⁸, F.A. Dias⁴⁶, M.A. Diaz^{32a}, E.B. Diehl⁸⁹, J. Dietrich¹⁶, S. Diglio⁸⁵, A. Dimitrievska¹³, J. Dingfelder²¹, P. Dita^{26a}, S. Dita^{26a}, F. Dittus³⁰, F. Djama⁸⁵, T. Djobava^{51b}, J.I. Djuvsland^{58a}, M.A.B. do Vale^{24c}, D. Dobos³⁰, M. Dobre^{26a}, C. Doglioni⁸¹, T. Dohmae¹⁵⁵, J. Dolejsi¹²⁹, Z. Dolezal¹²⁹, B.A. Dolgoshein^{98,*}, M. Donadelli^{24d}, S. Donati^{124a,124b}, P. Dondero^{121a,121b}, J. Donini³⁴, J. Dopke¹³¹, A. Doria^{104a}, M.T. Dova⁷¹, A.T. Doyle⁵³, E. Drechsler⁵⁴, M. Dris¹⁰, E. Dubreuil³⁴, E. Duchovni¹⁷², G. Duckeck¹⁰⁰, O.A. Ducu^{26a,85}, D. Duda¹⁰⁷, A. Dudarev³⁰, L. Duflot¹¹⁷, L. Duguid⁷⁷, M. Dührssen³⁰, M. Dunford^{58a}, H. Duran Yildiz^{4a}, M. Düren⁵², A. Durglishvili^{51b}, D. Duschinger⁴⁴, M. Dyndal^{38a}, C. Eckardt⁴², K.M. Ecker¹⁰¹, R.C. Edgar⁸⁹, W. Edson², N.C. Edwards⁴⁶, W. Ehrenfeld²¹, T. Eifert³⁰, G. Eigen¹⁴, K. Einsweiler¹⁵, T. Ekelof¹⁶⁶, M. El Kacimi^{135c}, M. Ellert¹⁶⁶, S. Elles⁵, F. Ellinghaus¹⁷⁵, A.A. Elliot¹⁶⁹, N. Ellis³⁰, J. Elmsheuser¹⁰⁰, M. Elsing³⁰, D. Emeliyanov¹³¹, Y. Enari¹⁵⁵, O.C. Endner⁸³, M. Endo¹¹⁸, J. Erdmann⁴³, A. Ereditato¹⁷, G. Ernis¹⁷⁵, J. Ernst², M. Ernst²⁵, S. Errede¹⁶⁵, E. Ertel⁸³, M. Escalier¹¹⁷, H. Esch⁴³, C. Escobar¹²⁵, B. Esposito⁴⁷, A.I. Etienne¹³⁶, E. Etzion¹⁵³, H. Evans⁶¹, A. Ezhilov¹²³, L. Fabbri^{20a,20b}, G. Facini³¹, R.M. Fakhrutdinov¹³⁰, S. Falciano^{132a}, R.J. Falla⁷⁸, J. Faltova¹²⁹, Y. Fang^{33a}, M. Fanti^{91a,91b}, A. Farbin⁸, A. Farilla^{134a}, T. Farooque¹², S. Farrell¹⁵, S.M. Farrington¹⁷⁰, P. Farthouat³⁰, F. Fassi^{135e}, P. Fassnacht³⁰, D. Fassouliotis⁹, M. Fucci Giannelli⁷⁷, A. Favareto^{50a,50b}, L. Fayard¹¹⁷, P. Federic^{144a}, O.L. Fedin^{123,m}, W. Fedorko¹⁶⁸, S. Feigl³⁰, L. Feligioni⁸⁵, C. Feng^{33d}, E.J. Feng⁶, H. Feng⁸⁹, A.B. Fenyuk¹³⁰, L. Feremenga⁸, P. Fernandez Martinez¹⁶⁷, S. Fernandez Perez³⁰, J. Ferrando⁵³, A. Ferrari¹⁶⁶, P. Ferrari¹⁰⁷, R. Ferrari^{121a}, D.E. Ferreira de Lima⁵³, A. Ferrer¹⁶⁷, D. Ferrere⁴⁹, C. Ferretti⁸⁹, A. Ferretto Parodi^{50a,50b}, M. Fiascaris³¹, F. Fiedler⁸³, A. Filipčič⁷⁵, M. Filipuzzi⁴², F. Filthaut¹⁰⁶, M. Fincke-Keeler¹⁶⁹, K.D. Finelli¹⁵⁰, M.C.N. Fiolhais^{126a,126c}, L. Fiorini¹⁶⁷, A. Firan⁴⁰, A. Fischer², C. Fischer¹², J. Fischer¹⁷⁵, W.C. Fisher⁹⁰, E.A. Fitzgerald²³, N. Flaschel⁴², I. Fleck¹⁴¹, P. Fleischmann⁸⁹, S. Fleischmann¹⁷⁵, G.T. Fletcher¹³⁹, G. Fletcher⁷⁶, R.R.M. Fletcher¹²², T. Flick¹⁷⁵, A. Floderus⁸¹, L.R. Flores Castillo^{60a}, M.J. Flowerdew¹⁰¹, A. Formica¹³⁶, A. Forti⁸⁴, D. Fournier¹¹⁷, H. Fox⁷², S. Fracchia¹², P. Francavilla⁸⁰, M. Franchini^{20a,20b}, D. Francis³⁰, L. Franconi¹¹⁹, M. Franklin⁵⁷, M. Frate¹⁶³, M. Fraternali^{121a,121b}, D. Freeborn⁷⁸, S.T. French²⁸, F. Friedrich⁴⁴, D. Froidevaux³⁰, J.A. Frost¹²⁰, C. Fukunaga¹⁵⁶, E. Fullana Torregrosa⁸³, B.G. Fulsom¹⁴³, T. Fusayasu¹⁰², J. Fuster¹⁶⁷, C. Gabaldon⁵⁵, O. Gabizon¹⁷⁵, A. Gabrielli^{20a,20b}, A. Gabrielli^{132a,132b}, G.P. Gach^{38a}, S. Gadatsch¹⁰⁷, S. Gadomski⁴⁹, G. Gagliardi^{50a,50b}, P. Gagnon⁶¹, C. Galea¹⁰⁶, B. Galhardo^{126a,126c}, E.J. Gallas¹²⁰, B.J. Gallop¹³¹, P. Gallus¹²⁸, G. Galster³⁶, K.K. Gan¹¹¹, J. Gao^{33b,85}, Y. Gao⁴⁶, Y.S. Gao^{143,e}, F.M. Garay Walls⁴⁶, F. Garberson¹⁷⁶, C. García¹⁶⁷, J.E. García Navarro¹⁶⁷, M. Garcia-Sciveres¹⁵, R.W. Gardner³¹, N. Garelli¹⁴³, V. Garonne¹¹⁹, C. Gatti⁴⁷, A. Gaudiello^{50a,50b}, G. Gaudio^{121a}, B. Gaur¹⁴¹,

L. Gauthier⁹⁵, P. Gauzzi^{132a,132b}, I.L. Gavrilenko⁹⁶, C. Gay¹⁶⁸, G. Gaycken²¹, E.N. Gazis¹⁰, P. Ge^{33d},
 Z. Gecse¹⁶⁸, C.N.P. Gee¹³¹, D.A.A. Geerts¹⁰⁷, Ch. Geich-Gimbel²¹, M.P. Geisler^{58a}, C. Gemme^{50a},
 M.H. Genest⁵⁵, S. Gentile^{132a,132b}, M. George⁵⁴, S. George⁷⁷, D. Gerbaudo¹⁶³, A. Gershon¹⁵³,
 S. Ghasemi¹⁴¹, H. Ghazlane^{135b}, B. Giacobbe^{20a}, S. Giagu^{132a,132b}, V. Giangiobbe¹²,
 P. Giannetti^{124a,124b}, B. Gibbard²⁵, S.M. Gibson⁷⁷, M. Gilchriese¹⁵, T.P.S. Gillam²⁸, D. Gillberg³⁰,
 G. Gilles³⁴, D.M. Gingrich^{3,d}, N. Giokaris⁹, M.P. Giordani^{164a,164c}, F.M. Giorgi^{20a}, F.M. Giorgi¹⁶,
 P.F. Giraud¹³⁶, P. Giromini⁴⁷, D. Giugni^{91a}, C. Giuliani⁴⁸, M. Giulini^{58b}, B.K. Gjelsten¹¹⁹,
 S. Gkaitatzis¹⁵⁴, I. Gkialas¹⁵⁴, E.L. Gkougkousis¹¹⁷, L.K. Gladilin⁹⁹, C. Glasman⁸², J. Glatzer³⁰,
 P.C.F. Glashyshen⁴⁶, A. Glazov⁴², M. Goblirsch-Kolb¹⁰¹, J.R. Goddard⁷⁶, J. Godlewski³⁹, S. Goldfarb⁸⁹,
 T. Golling⁴⁹, D. Golubkov¹³⁰, A. Gomes^{126a,126b,126d}, R. Gonçalo^{126a},
 J. Goncalves Pinto Firmino Da Costa¹³⁶, L. Gonella²¹, S. González de la Hoz¹⁶⁷, G. Gonzalez Parra¹²,
 S. Gonzalez-Sevilla⁴⁹, L. Goossens³⁰, P.A. Gorbounov⁹⁷, H.A. Gordon²⁵, I. Gorelov¹⁰⁵, B. Gorini³⁰,
 E. Gorini^{73a,73b}, A. Gorišek⁷⁵, E. Gornicki³⁹, A.T. Goshaw⁴⁵, C. Gössling⁴³, M.I. Gostkin⁶⁵,
 D. Goujdami^{135c}, A.G. Goussiou¹³⁸, N. Govender^{145b}, E. Gozani¹⁵², H.M.X. Grabas¹³⁷, L. Gruber⁵⁴,
 I. Grabowska-Bold^{38a}, P.O.J. Gradin¹⁶⁶, P. Grafström^{20a,20b}, K-J. Grahn⁴², J. Gramling⁴⁹,
 E. Gramstad¹¹⁹, S. Grancagnolo¹⁶, V. Grassi¹⁴⁸, V. Gratchev¹²³, H.M. Gray³⁰, E. Graziani^{134a},
 Z.D. Greenwood^{79,n}, K. Gregersen⁷⁸, I.M. Gregor⁴², P. Grenier¹⁴³, J. Griffiths⁸, A.A. Grillo¹³⁷,
 K. Grimm⁷², S. Grinstein^{12,o}, Ph. Gris³⁴, J.-F. Grivaz¹¹⁷, J.P. Grohs⁴⁴, A. Grohsjean⁴², E. Gross¹⁷²,
 J. Grosse-Knetter⁵⁴, G.C. Grossi⁷⁹, Z.J. Grout¹⁴⁹, L. Guan⁸⁹, J. Guenther¹²⁸, F. Guescini⁴⁹, D. Guest¹⁷⁶,
 O. Gueta¹⁵³, E. Guido^{50a,50b}, T. Guillemin¹¹⁷, S. Guindon², U. Gul⁵³, C. Gumpert⁴⁴, J. Guo^{33e},
 Y. Guo^{33b}, S. Gupta¹²⁰, G. Gustavino^{132a,132b}, P. Gutierrez¹¹³, N.G. Gutierrez Ortiz⁷⁸, C. Gutschow⁴⁴,
 C. Guyot¹³⁶, C. Gwenlan¹²⁰, C.B. Gwilliam⁷⁴, A. Haas¹¹⁰, C. Haber¹⁵, H.K. Hadavand⁸, N. Haddad^{135e},
 P. Haefner²¹, S. Hageböck²¹, Z. Hajduk³⁹, H. Hakobyan¹⁷⁷, M. Haleem⁴², J. Haley¹¹⁴, D. Hall¹²⁰,
 G. Halladjian⁹⁰, G.D. Hallewell⁸⁵, K. Hamacher¹⁷⁵, P. Hamal¹¹⁵, K. Hamano¹⁶⁹, M. Hamer⁵⁴,
 A. Hamilton^{145a}, G.N. Hamity^{145c}, P.G. Hamnett⁴², L. Han^{33b}, K. Hanagaki⁶⁶, K. Hanawa¹⁵⁵,
 M. Hance¹⁵, P. Hanke^{58a}, R. Hanna¹³⁶, J.B. Hansen³⁶, J.D. Hansen³⁶, M.C. Hansen²¹, P.H. Hansen³⁶,
 K. Hara¹⁶⁰, A.S. Hard¹⁷³, T. Harenberg¹⁷⁵, F. Hariri¹¹⁷, S. Harkusha⁹², R.D. Harrington⁴⁶,
 P.F. Harrison¹⁷⁰, F. Hartjes¹⁰⁷, M. Hasegawa⁶⁷, S. Hasegawa¹⁰³, Y. Hasegawa¹⁴⁰, A. Hasib¹¹³,
 S. Hassani¹³⁶, S. Haug¹⁷, R. Hauser⁹⁰, L. Hauswald⁴⁴, M. Havranek¹²⁷, C.M. Hawkes¹⁸,
 R.J. Hawkings³⁰, A.D. Hawkins⁸¹, T. Hayashi¹⁶⁰, D. Hayden⁹⁰, C.P. Hays¹²⁰, J.M. Hays⁷⁶,
 H.S. Hayward⁷⁴, S.J. Haywood¹³¹, S.J. Head¹⁸, T. Heck⁸³, V. Hedberg⁸¹, L. Heelan⁸, S. Heim¹²²,
 T. Heim¹⁷⁵, B. Heinemann¹⁵, L. Heinrich¹¹⁰, J. Hejbal¹²⁷, L. Helary²², S. Hellman^{146a,146b},
 D. Hellmich²¹, C. Helsens¹², J. Henderson¹²⁰, R.C.W. Henderson⁷², Y. Heng¹⁷³, C. Hengler⁴²,
 A. Henrichs¹⁷⁶, A.M. Henriques Correia³⁰, S. Henrot-Versille¹¹⁷, G.H. Herbert¹⁶,
 Y. Hernández Jiménez¹⁶⁷, R. Herrberg-Schubert¹⁶, G. Herten⁴⁸, R. Hertenberger¹⁰⁰, L. Hervas³⁰,
 G.G. Hesketh⁷⁸, N.P. Hessey¹⁰⁷, J.W. Hetherly⁴⁰, R. Hickling⁷⁶, E. Higón-Rodriguez¹⁶⁷, E. Hill¹⁶⁹,
 J.C. Hill²⁸, K.H. Hiller⁴², S.J. Hillier¹⁸, I. Hinchliffe¹⁵, E. Hines¹²², R.R. Hinman¹⁵, M. Hirose¹⁵⁷,
 D. Hirschbuehl¹⁷⁵, J. Hobbs¹⁴⁸, N. Hod¹⁰⁷, M.C. Hodgkinson¹³⁹, P. Hodgson¹³⁹, A. Hoecker³⁰,
 M.R. Hoeferkamp¹⁰⁵, F. Hoenig¹⁰⁰, M. Hohlfeld⁸³, D. Hohn²¹, T.R. Holmes¹⁵, M. Homann⁴³,
 T.M. Hong¹²⁵, L. Hooft van Huysduynen¹¹⁰, W.H. Hopkins¹¹⁶, Y. Horii¹⁰³, A.J. Horton¹⁴²,
 J.-Y. Hostachy⁵⁵, S. Hou¹⁵¹, A. Hoummada^{135a}, J. Howard¹²⁰, J. Howarth⁴², M. Hrabovsky¹¹⁵,
 I. Hristova¹⁶, J. Hrvnac¹¹⁷, T. Hrynn'ova⁵, A. Hrynevich⁹³, C. Hsu^{145c}, P.J. Hsu^{151,p}, S.-C. Hsu¹³⁸,
 D. Hu³⁵, Q. Hu^{33b}, X. Hu⁸⁹, Y. Huang⁴², Z. Hubacek¹²⁸, F. Hubaut⁸⁵, F. Huegging²¹, T.B. Huffman¹²⁰,
 E.W. Hughes³⁵, G. Hughes⁷², M. Huhtinen³⁰, T.A. Hülsing⁸³, N. Huseynov^{65,b}, J. Huston⁹⁰, J. Huth⁵⁷,
 G. Iacobucci⁴⁹, G. Iakovidis²⁵, I. Ibragimov¹⁴¹, L. Iconomidou-Fayard¹¹⁷, E. Ideal¹⁷⁶, Z. Idrissi^{135e},
 P. Iengo³⁰, O. Igonkina¹⁰⁷, T. Iizawa¹⁷¹, Y. Ikegami⁶⁶, K. Ikematsu¹⁴¹, M. Ikeno⁶⁶, Y. Ilchenko^{31,q},
 D. Iliadis¹⁵⁴, N. Ilic¹⁴³, T. Ince¹⁰¹, G. Introzzi^{121a,121b}, P. Ioannou⁹, M. Iodice^{134a}, K. Iordanidou³⁵,

V. Ippolito⁵⁷, A. Irles Quiles¹⁶⁷, C. Isaksson¹⁶⁶, M. Ishino⁶⁸, M. Ishitsuka¹⁵⁷, R. Ishmukhametov¹¹¹, C. Issever¹²⁰, S. Isti^{19a}, J.M. Iturbe Ponce⁸⁴, R. Iuppa^{133a,133b}, J. Ivarsson⁸¹, W. Iwanski³⁹, H. Iwasaki⁶⁶, J.M. Izen⁴¹, V. Izzo^{104a}, S. Jabbar³, B. Jackson¹²², M. Jackson⁷⁴, P. Jackson¹, M.R. Jaekel³⁰, V. Jain², K. Jakobs⁴⁸, S. Jakobsen³⁰, T. Jakoubek¹²⁷, J. Jakubek¹²⁸, D.O. Jamin¹¹⁴, D.K. Jana⁷⁹, E. Jansen⁷⁸, R. Jansky⁶², J. Janssen²¹, M. Janus¹⁷⁰, G. Jarlskog⁸¹, N. Javadov^{65,b}, T. Javůrek⁴⁸, L. Jeanty¹⁵, J. Jejelava^{51a,r}, G.-Y. Jeng¹⁵⁰, D. Jennens⁸⁸, P. Jenni^{48,s}, J. Jentzsch⁴³, C. Jeske¹⁷⁰, S. Jézéquel⁵, H. Ji¹⁷³, J. Jia¹⁴⁸, Y. Jiang^{33b}, S. Jiggins⁷⁸, J. Jimenez Pena¹⁶⁷, S. Jin^{33a}, A. Jinaru^{26a}, O. Jinnouchi¹⁵⁷, M.D. Joergensen³⁶, P. Johansson¹³⁹, K.A. Johns⁷, K. Jon-And^{146a,146b}, G. Jones¹⁷⁰, R.W.L. Jones⁷², T.J. Jones⁷⁴, J. Jongmanns^{58a}, P.M. Jorge^{126a,126b}, K.D. Joshi⁸⁴, J. Jovicevic^{159a}, X. Ju¹⁷³, C.A. Jung⁴³, P. Jussel⁶², A. Juste Rozas^{12,o}, M. Kaci¹⁶⁷, A. Kaczmarska³⁹, M. Kado¹¹⁷, H. Kagan¹¹¹, M. Kagan¹⁴³, S.J. Kahn⁸⁵, E. Kajomovitz⁴⁵, C.W. Kalderon¹²⁰, S. Kama⁴⁰, A. Kamenshchikov¹³⁰, N. Kanaya¹⁵⁵, S. Kaneti²⁸, V.A. Kantserov⁹⁸, J. Kanzaki⁶⁶, B. Kaplan¹¹⁰, L.S. Kaplan¹⁷³, A. Kapliy³¹, D. Kar⁵³, K. Karakostas¹⁰, A. Karamaoun³, N. Karastathis^{10,107}, M.J. Kareem⁵⁴, E. Karentzos¹⁰, M. Karnevskiy⁸³, S.N. Karpov⁶⁵, Z.M. Karpova⁶⁵, K. Karthik¹¹⁰, V. Kartvelishvili⁷², A.N. Karyukhin¹³⁰, L. Kashif¹⁷³, R.D. Kass¹¹¹, A. Kastanas¹⁴, Y. Kataoka¹⁵⁵, C. Kato¹⁵⁵, A. Katre⁴⁹, J. Katzy⁴², K. Kawagoe⁷⁰, T. Kawamoto¹⁵⁵, G. Kawamura⁵⁴, S. Kazama¹⁵⁵, V.F. Kazanin^{109,c}, R. Keeler¹⁶⁹, R. Kehoe⁴⁰, J.S. Keller⁴², J.J. Kempster⁷⁷, H. Keoshkerian⁸⁴, O. Kepka¹²⁷, B.P. Kerševan⁷⁵, S. Kersten¹⁷⁵, R.A. Keyes⁸⁷, F. Khalil-zada¹¹, H. Khandanyan^{146a,146b}, A. Khanov¹¹⁴, A.G. Kharlamov^{109,c}, T.J. Khoo²⁸, V. Khovanskiy⁹⁷, E. Khramov⁶⁵, J. Khubua^{51b,t}, H.Y. Kim⁸, H. Kim^{146a,146b}, S.H. Kim¹⁶⁰, Y. Kim³¹, N. Kimura¹⁵⁴, O.M. Kind¹⁶, B.T. King⁷⁴, M. King¹⁶⁷, S.B. King¹⁶⁸, J. Kirk¹³¹, A.E. Kiryunin¹⁰¹, T. Kishimoto⁶⁷, D. Kisielewska^{38a}, F. Kiss⁴⁸, K. Kiuchi¹⁶⁰, O. Kivernyk¹³⁶, E. Kladiva^{144b}, M.H. Klein³⁵, M. Klein⁷⁴, U. Klein⁷⁴, K. Kleinknecht⁸³, P. Klimek^{146a,146b}, A. Klimentov²⁵, R. Klingenberg⁴³, J.A. Klinger¹³⁹, T. Klioutchnikova³⁰, E.-E. Kluge^{58a}, P. Kluit¹⁰⁷, S. Kluth¹⁰¹, J. Knapik³⁹, E. Kneringer⁶², E.B.F.G. Knoops⁸⁵, A. Knue⁵³, A. Kobayashi¹⁵⁵, D. Kobayashi¹⁵⁷, T. Kobayashi¹⁵⁵, M. Kobel⁴⁴, M. Kocian¹⁴³, P. Kodys¹²⁹, T. Koffas²⁹, E. Koffeman¹⁰⁷, L.A. Kogan¹²⁰, S. Kohlmann¹⁷⁵, Z. Kohout¹²⁸, T. Kohriki⁶⁶, T. Koi¹⁴³, H. Kolanoski¹⁶, I. Koletsou⁵, A.A. Komar^{96,*}, Y. Komori¹⁵⁵, T. Kondo⁶⁶, N. Kondrashova⁴², K. Köneke⁴⁸, A.C. König¹⁰⁶, T. Kono⁶⁶, R. Konoplich^{110,u}, N. Konstantinidis⁷⁸, R. Kopeliansky¹⁵², S. Koperny^{38a}, L. Köpke⁸³, A.K. Kopp⁴⁸, K. Korcyl³⁹, K. Kordas¹⁵⁴, A. Korn⁷⁸, A.A. Korol^{109,c}, I. Korolkov¹², E.V. Korolkova¹³⁹, O. Kortner¹⁰¹, S. Kortner¹⁰¹, T. Kosek¹²⁹, V.V. Kostyukhin²¹, V.M. Kotov⁶⁵, A. Kotwal⁴⁵, A. Kourkoumeli-Charalampidi¹⁵⁴, C. Kourkoumelis⁹, V. Kouskoura²⁵, A. Koutsman^{159a}, R. Kowalewski¹⁶⁹, T.Z. Kowalski^{38a}, W. Kozanecki¹³⁶, A.S. Kozhin¹³⁰, V.A. Kramarenko⁹⁹, G. Kramberger⁷⁵, D. Krasnoperovtsev⁹⁸, M.W. Krasny⁸⁰, A. Krasznahorkay³⁰, J.K. Kraus²¹, A. Kravchenko²⁵, S. Kreiss¹¹⁰, M. Kretz^{58c}, J. Kretzschmar⁷⁴, K. Kreutzfeldt⁵², P. Krieger¹⁵⁸, K. Krizka³¹, K. Kroeninger⁴³, H. Kroha¹⁰¹, J. Kroll¹²², J. Kroseberg²¹, J. Krstic¹³, U. Kruchonak⁶⁵, H. Krüger²¹, N. Krumnack⁶⁴, A. Kruse¹⁷³, M.C. Kruse⁴⁵, M. Kruskal²², T. Kubota⁸⁸, H. Kucuk⁷⁸, S. Kuday^{4b}, S. Kuehn⁴⁸, A. Kugel^{58c}, F. Kuger¹⁷⁴, A. Kuhl¹³⁷, T. Kuhl⁴², V. Kukhtin⁶⁵, Y. Kulchitsky⁹², S. Kuleshov^{32b}, M. Kuna^{132a,132b}, T. Kunigo⁶⁸, A. Kupco¹²⁷, H. Kurashige⁶⁷, Y.A. Kurochkin⁹², V. Kus¹²⁷, E.S. Kuwertz¹⁶⁹, M. Kuze¹⁵⁷, J. Kvita¹¹⁵, T. Kwan¹⁶⁹, D. Kyriazopoulos¹³⁹, A. La Rosa¹³⁷, J.L. La Rosa Navarro^{24d}, L. La Rotonda^{37a,37b}, C. Lacasta¹⁶⁷, F. Lacava^{132a,132b}, J. Lacey²⁹, H. Lacker¹⁶, D. Lacour⁸⁰, V.R. Lacuesta¹⁶⁷, E. Ladygin⁶⁵, R. Lafaye⁵, B. Laforge⁸⁰, T. Lagouri¹⁷⁶, S. Lai⁵⁴, L. Lambourne⁷⁸, S. Lammers⁶¹, C.L. Lampen⁷, W. Lampl⁷, E. Lançon¹³⁶, U. Landgraf⁴⁸, M.P.J. Landon⁷⁶, V.S. Lang^{58a}, J.C. Lange¹², A.J. Lankford¹⁶³, F. Lanni²⁵, K. Lantzsch³⁰, A. Lanza^{121a}, S. Laplace⁸⁰, C. Lapoire³⁰, J.F. Laporte¹³⁶, T. Lari^{91a}, F. Lasagni Manghi^{20a,20b}, M. Lassnig³⁰, P. Laurelli⁴⁷, W. Lavrijssen¹⁵, A.T. Law¹³⁷, P. Laycock⁷⁴, T. Lazovich⁵⁷, O. Le Dortz⁸⁰, E. Le Guiriec⁸⁵, E. Le Menedeu¹², M. LeBlanc¹⁶⁹, T. LeCompte⁶, F. Ledroit-Guillon⁵⁵, C.A. Lee^{145b}, S.C. Lee¹⁵¹, L. Lee¹, G. Lefebvre⁸⁰, M. Lefebvre¹⁶⁹, F. Leggett¹⁰⁰, C. Leggett¹⁵, A. Lehan⁷⁴, G. Lehmann Miotto³⁰,

X. Lei⁷, W.A. Leight²⁹, A. Leisos^{154,v}, A.G. Leister¹⁷⁶, M.A.L. Leite^{24d}, R. Leitner¹²⁹, D. Lellouch¹⁷², B. Lemmer⁵⁴, K.J.C. Leney⁷⁸, T. Lenz²¹, B. Lenzi³⁰, R. Leone⁷, S. Leone^{124a,124b}, C. Leonidopoulos⁴⁶, S. Leontsinis¹⁰, C. Leroy⁹⁵, C.G. Lester²⁸, M. Levchenko¹²³, J. Levêque⁵, D. Levin⁸⁹, L.J. Levinson¹⁷², M. Levy¹⁸, A. Lewis¹²⁰, A.M. Leyko²¹, M. Leyton⁴¹, B. Li^{33b,w}, H. Li¹⁴⁸, H.L. Li³¹, L. Li⁴⁵, L. Li^{33e}, S. Li⁴⁵, Y. Li^{33c,x}, Z. Liang¹³⁷, H. Liao³⁴, B. Liberti^{133a}, A. Liblong¹⁵⁸, P. Lichard³⁰, K. Lie¹⁶⁵, J. Liebal²¹, W. Liebig¹⁴, C. Limbach²¹, A. Limosani¹⁵⁰, S.C. Lin^{151,y}, T.H. Lin⁸³, F. Linde¹⁰⁷, B.E. Lindquist¹⁴⁸, J.T. Linnemann⁹⁰, E. Lipeles¹²², A. Lipniacka¹⁴, M. Lisovyi^{58b}, T.M. Liss¹⁶⁵, D. Lissauer²⁵, A. Lister¹⁶⁸, A.M. Litke¹³⁷, B. Liu^{151,z}, D. Liu¹⁵¹, H. Liu⁸⁹, J. Liu⁸⁵, J.B. Liu^{33b}, K. Liu⁸⁵, L. Liu¹⁶⁵, M. Liu⁴⁵, M. Liu^{33b}, Y. Liu^{33b}, M. Livan^{121a,121b}, A. Lleres⁵⁵, J. Llorente Merino⁸², S.L. Lloyd⁷⁶, F. Lo Sterzo¹⁵¹, E. Lobodzinska⁴², P. Loch⁷, W.S. Lockman¹³⁷, F.K. Loebinger⁸⁴, A.E. Loevschall-Jensen³⁶, A. Loginov¹⁷⁶, T. Lohse¹⁶, K. Lohwasser⁴², M. Lokajicek¹²⁷, B.A. Long²², J.D. Long⁸⁹, R.E. Long⁷², K.A.Looper¹¹¹, L. Lopes^{126a}, D. Lopez Mateos⁵⁷, B. Lopez Paredes¹³⁹, I. Lopez Paz¹², J. Lorenz¹⁰⁰, N. Lorenzo Martinez⁶¹, M. Losada¹⁶², P. Loscutoff¹⁵, P.J. Lösel¹⁰⁰, X. Lou^{33a}, A. Lounis¹¹⁷, J. Love⁶, P.A. Love⁷², N. Lu⁸⁹, H.J. Lubatti¹³⁸, C. Luci^{132a,132b}, A. Lucotte⁵⁵, F. Luehring⁶¹, W. Lukas⁶², L. Luminari^{132a}, O. Lundberg^{146a,146b}, B. Lund-Jensen¹⁴⁷, D. Lynn²⁵, R. Lysak¹²⁷, E. Lytken⁸¹, H. Ma²⁵, L.L. Ma^{33d}, G. Maccarrone⁴⁷, A. Macchiolo¹⁰¹, C.M. Macdonald¹³⁹, J. Machado Miguens^{122,126b}, D. Macina³⁰, D. Madaffari⁸⁵, R. Madar³⁴, H.J. Maddocks⁷², W.F. Mader⁴⁴, A. Madsen¹⁶⁶, S. Maeland¹⁴, T. Maeno²⁵, A. Maevskiy⁹⁹, E. Magradze⁵⁴, K. Mahboubi⁴⁸, J. Mahlstedt¹⁰⁷, C. Maiani¹³⁶, C. Maidantchik^{24a}, A.A. Maier¹⁰¹, T. Maier¹⁰⁰, A. Maio^{126a,126b,126d}, S. Majewski¹¹⁶, Y. Makida⁶⁶, N. Makovec¹¹⁷, B. Malaescu⁸⁰, Pa. Malecki³⁹, V.P. Maleev¹²³, F. Malek⁵⁵, U. Mallik⁶³, D. Malon⁶, C. Malone¹⁴³, S. Maltezos¹⁰, V.M. Malyshев¹⁰⁹, S. Malyukov³⁰, J. Mamuzic⁴², G. Mancini⁴⁷, B. Mandelli³⁰, L. Mandelli^{91a}, I. Mandić⁷⁵, R. Mandrysch⁶³, J. Maneira^{126a,126b}, A. Manfredini¹⁰¹, L. Manhaes de Andrade Filho^{24b}, J. Manjarres Ramos^{159b}, A. Mann¹⁰⁰, P.M. Manning¹³⁷, A. Manousakis-Katsikakis⁹, B. Mansoulie¹³⁶, R. Mantifel⁸⁷, M. Mantoani⁵⁴, L. Mapelli³⁰, L. March^{145c}, G. Marchiori⁸⁰, M. Marcisovsky¹²⁷, C.P. Marino¹⁶⁹, M. Marjanovic¹³, D.E. Marley⁸⁹, F. Marroquim^{24a}, S.P. Marsden⁸⁴, Z. Marshall¹⁵, L.F. Marti¹⁷, S. Marti-Garcia¹⁶⁷, B. Martin⁹⁰, T.A. Martin¹⁷⁰, V.J. Martin⁴⁶, B. Martin dit Latour¹⁴, M. Martinez^{12,o}, S. Martin-Haugh¹³¹, V.S. Martouï^{26a}, A.C. Martyniuk⁷⁸, M. Marx¹³⁸, F. Marzano^{132a}, A. Marzin³⁰, L. Masetti⁸³, T. Mashimo¹⁵⁵, R. Mashinistov⁹⁶, J. Masik⁸⁴, A.L. Maslenikov^{109,c}, I. Massa^{20a,20b}, L. Massa^{20a,20b}, N. Massol⁵, P. Mastrandrea¹⁴⁸, A. Mastroberardino^{37a,37b}, T. Masubuchi¹⁵⁵, P. Mättig¹⁷⁵, J. Mattmann⁸³, J. Maurer^{26a}, S.J. Maxfield⁷⁴, D.A. Maximov^{109,c}, R. Mazini¹⁵¹, S.M. Mazza^{91a,91b}, L. Mazzaferro^{133a,133b}, G. Mc Goldrick¹⁵⁸, S.P. Mc Kee⁸⁹, A. McCarn⁸⁹, R.L. McCarthy¹⁴⁸, T.G. McCarthy²⁹, N.A. McCubbin¹³¹, K.W. McFarlane^{56,*}, J.A. McFayden⁷⁸, G. Mchedlidze⁵⁴, S.J. McMahon¹³¹, R.A. McPherson^{169,k}, M. Medinnis⁴², S. Meehan^{145a}, S. Mehlhase¹⁰⁰, A. Mehta⁷⁴, K. Meier^{58a}, C. Meineck¹⁰⁰, B. Meirose⁴¹, B.R. Mellado Garcia^{145c}, F. Meloni¹⁷, A. Mengarelli^{20a,20b}, S. Menke¹⁰¹, E. Meoni¹⁶¹, K.M. Mercurio⁵⁷, S. Mergelmeyer²¹, P. Mermod⁴⁹, L. Merola^{104a,104b}, C. Meroni^{91a}, F.S. Merritt³¹, A. Messina^{132a,132b}, J. Metcalfe²⁵, A.S. Mete¹⁶³, C. Meyer⁸³, C. Meyer¹²², J.-P. Meyer¹³⁶, J. Meyer¹⁰⁷, R.P. Middleton¹³¹, S. Miglioranzi^{164a,164c}, L. Mijović²¹, G. Mikenberg¹⁷², M. Mikestikova¹²⁷, M. Mikuž⁷⁵, M. Milesi⁸⁸, A. Milic³⁰, D.W. Miller³¹, C. Mills⁴⁶, A. Milov¹⁷², D.A. Milstead^{146a,146b}, A.A. Minaenko¹³⁰, Y. Minami¹⁵⁵, I.A. Minashvili⁶⁵, A.I. Mincer¹¹⁰, B. Mindur^{38a}, M. Mineev⁶⁵, Y. Ming¹⁷³, L.M. Mir¹², T. Mitani¹⁷¹, J. Mitrevski¹⁰⁰, V.A. Mitsou¹⁶⁷, A. Miucci⁴⁹, P.S. Miyagawa¹³⁹, J.U. Mjörnmark⁸¹, T. Moa^{146a,146b}, K. Mochizuki⁸⁵, S. Mohapatra³⁵, W. Mohr⁴⁸, S. Molander^{146a,146b}, R. Moles-Valls²¹, K. Mönig⁴², C. Monini⁵⁵, J. Monk³⁶, E. Monnier⁸⁵, J. Montejo Berlingen¹², F. Monticelli⁷¹, S. Monzani^{132a,132b}, R.W. Moore³, N. Morange¹¹⁷, D. Moreno¹⁶², M. Moreno Llácer⁵⁴, P. Morettini^{50a}, M. Morgenstern⁴⁴, D. Mori¹⁴², M. Morii⁵⁷, M. Morinaga¹⁵⁵, V. Morisbak¹¹⁹, S. Moritz⁸³, A.K. Morley¹⁵⁰, G. Mornacchi³⁰, J.D. Morris⁷⁶, S.S. Mortensen³⁶, A. Morton⁵³, L. Morvaj¹⁰³, M. Mosidze^{51b}, J. Moss¹¹¹, K. Motohashi¹⁵⁷,

R. Mount¹⁴³, E. Mountricha²⁵, S.V. Mouraviev^{96,*}, E.J.W. Moyse⁸⁶, S. Muanza⁸⁵, R.D. Mudd¹⁸, F. Mueller¹⁰¹, J. Mueller¹²⁵, R.S.P. Mueller¹⁰⁰, T. Mueller²⁸, D. Muenstermann⁴⁹, P. Mullen⁵³, G.A. Mullier¹⁷, J.A. Murillo Quijada¹⁸, W.J. Murray^{170,131}, H. Musheghyan⁵⁴, E. Musto¹⁵², A.G. Myagkov^{130,aa}, M. Myska¹²⁸, B.P. Nachman¹⁴³, O. Nackenhorst⁵⁴, J. Nadal⁵⁴, K. Nagai¹²⁰, R. Nagai¹⁵⁷, Y. Nagai⁸⁵, K. Nagano⁶⁶, A. Nagarkar¹¹¹, Y. Nagasaka⁵⁹, K. Nagata¹⁶⁰, M. Nagel¹⁰¹, E. Nagy⁸⁵, A.M. Nairz³⁰, Y. Nakahama³⁰, K. Nakamura⁶⁶, T. Nakamura¹⁵⁵, I. Nakano¹¹², H. Namasivayam⁴¹, R.F. Naranjo Garcia⁴², R. Narayan³¹, T. Naumann⁴², G. Navarro¹⁶², R. Nayyar⁷, H.A. Neal⁸⁹, P.Yu. Nechaeva⁹⁶, T.J. Neep⁸⁴, P.D. Nef¹⁴³, A. Negri^{121a,121b}, M. Negrini^{20a}, S. Nektarijevic¹⁰⁶, C. Nellist¹¹⁷, A. Nelson¹⁶³, S. Nemecek¹²⁷, P. Nemethy¹¹⁰, A.A. Nepomuceno^{24a}, M. Nessi^{30,ab}, M.S. Neubauer¹⁶⁵, M. Neumann¹⁷⁵, R.M. Neves¹¹⁰, P. Nevski²⁵, P.R. Newman¹⁸, D.H. Nguyen⁶, R.B. Nickerson¹²⁰, R. Nicolaïdou¹³⁶, B. Nicquevert³⁰, J. Nielsen¹³⁷, N. Nikiforou³⁵, A. Nikiforov¹⁶, V. Nikolaenko^{130,aa}, I. Nikolic-Audit⁸⁰, K. Nikolopoulos¹⁸, J.K. Nilsen¹¹⁹, P. Nilsson²⁵, Y. Ninomiya¹⁵⁵, A. Nisati^{132a}, R. Nisius¹⁰¹, T. Nobe¹⁵⁵, M. Nomachi¹¹⁸, I. Nomidis²⁹, T. Nooney⁷⁶, S. Norberg¹¹³, M. Nordberg³⁰, O. Novgorodova⁴⁴, S. Nowak¹⁰¹, M. Nozaki⁶⁶, L. Nozka¹¹⁵, K. Ntekas¹⁰, G. Nunes Hanninger⁸⁸, T. Nunnemann¹⁰⁰, E. Nurse⁷⁸, F. Nuti⁸⁸, B.J. O'Brien⁴⁶, F. O'grady⁷, D.C. O'Neil¹⁴², V. O'Shea⁵³, F.G. Oakham^{29,d}, H. Oberlack¹⁰¹, T. Obermann²¹, J. Ocariz⁸⁰, A. Ochi⁶⁷, I. Ochoa⁷⁸, J.P. Ochoa-Ricoux^{32a}, S. Oda⁷⁰, S. Odaka⁶⁶, H. Ogren⁶¹, A. Oh⁸⁴, S.H. Oh⁴⁵, C.C. Ohm¹⁵, H. Ohman¹⁶⁶, H. Oide³⁰, W. Okamura¹¹⁸, H. Okawa¹⁶⁰, Y. Okumura³¹, T. Okuyama⁶⁶, A. Olariu^{26a}, S.A. Olivares Pino⁴⁶, D. Oliveira Damazio²⁵, E. Oliver Garcia¹⁶⁷, A. Olszewski³⁹, J. Olszowska³⁹, A. Onofre^{126a,126e}, P.U.E. Onyisi^{31,q}, C.J. Oram^{159a}, M.J. Oreglia³¹, Y. Oren¹⁵³, D. Orestano^{134a,134b}, N. Orlando¹⁵⁴, C. Oropeza Barrera⁵³, R.S. Orr¹⁵⁸, B. Osculati^{50a,50b}, R. Ospanov⁸⁴, G. Otero y Garzon²⁷, H. Otono⁷⁰, M. Ouchrif^{135d}, E.A. Ouellette¹⁶⁹, F. Ould-Saada¹¹⁹, A. Ouraou¹³⁶, K.P. Oussoren¹⁰⁷, Q. Ouyang^{33a}, A. Ovcharova¹⁵, M. Owen⁵³, R.E. Owen¹⁸, V.E. Ozcan^{19a}, N. Ozturk⁸, K. Pachal¹⁴², A. Pacheco Pages¹², C. Padilla Aranda¹², M. Pagáčová⁴⁸, S. Pagan Griso¹⁵, E. Paganis¹³⁹, F. Paige²⁵, P. Pais⁸⁶, K. Pajchel¹¹⁹, G. Palacino^{159b}, S. Palestini³⁰, M. Palka^{38b}, D. Pallin³⁴, A. Palma^{126a,126b}, Y.B. Pan¹⁷³, E. Panagiotopoulou¹⁰, C.E. Pandini⁸⁰, J.G. Panduro Vazquez⁷⁷, P. Pani^{146a,146b}, S. Panitkin²⁵, D. Pantea^{26a}, L. Paolozzi⁴⁹, Th.D. Papadopoulou¹⁰, K. Papageorgiou¹⁵⁴, A. Paramonov⁶, D. Paredes Hernandez¹⁵⁴, M.A. Parker²⁸, K.A. Parker¹³⁹, F. Parodi^{50a,50b}, J.A. Parsons³⁵, U. Parzefall⁴⁸, E. Pasqualucci^{132a}, S. Passaggio^{50a}, F. Pastore^{134a,134b,*}, Fr. Pastore⁷⁷, G. Pásztor²⁹, S. Pataraia¹⁷⁵, N.D. Patel¹⁵⁰, J.R. Pater⁸⁴, T. Pauly³⁰, J. Pearce¹⁶⁹, B. Pearson¹¹³, L.E. Pedersen³⁶, M. Pedersen¹¹⁹, S. Pedraza Lopez¹⁶⁷, R. Pedro^{126a,126b}, S.V. Peleganchuk^{109,c}, D. Pelikan¹⁶⁶, O. Penc¹²⁷, C. Peng^{33a}, H. Peng^{33b}, B. Penning³¹, J. Penwell⁶¹, D.V. Perepelitsa²⁵, E. Perez Codina^{159a}, M.T. Pérez García-Estañ¹⁶⁷, L. Perini^{91a,91b}, H. Pernegger³⁰, S. Perrella^{104a,104b}, R. Peschke⁴², V.D. Peshekhanov⁶⁵, K. Peters³⁰, R.F.Y. Peters⁸⁴, B.A. Petersen³⁰, T.C. Petersen³⁶, E. Petit⁴², A. Petridis^{146a,146b}, C. Petridou¹⁵⁴, P. Petroff¹¹⁷, E. Petrolo^{132a}, F. Petrucci^{134a,134b}, N.E. Pettersson¹⁵⁷, R. Pezoa^{32b}, P.W. Phillips¹³¹, G. Piacquadio¹⁴³, E. Pianori¹⁷⁰, A. Picazio⁴⁹, E. Piccaro⁷⁶, M. Piccinini^{20a,20b}, M.A. Pickering¹²⁰, R. Piegala²⁷, D.T. Pignotti¹¹¹, J.E. Pilcher³¹, A.D. Pilkington⁸⁴, J. Pina^{126a,126b,126d}, M. Pinamonti^{164a,164c,ac}, J.L. Pinfold³, A. Pingel³⁶, B. Pinto^{126a}, S. Pires⁸⁰, H. Pirumov⁴², M. Pitt¹⁷², C. Pizio^{91a,91b}, L. Plazak^{144a}, M.-A. Pleier²⁵, V. Pleskot¹²⁹, E. Plotnikova⁶⁵, P. Plucinski^{146a,146b}, D. Pluth⁶⁴, R. Poettgen^{146a,146b}, L. Poggioli¹¹⁷, D. Pohl²¹, G. Polesello^{121a}, A. Poley⁴², A. Pollicchio^{37a,37b}, R. Polifka¹⁵⁸, A. Polini^{20a}, C.S. Pollard⁵³, V. Polychronakos²⁵, K. Pommès³⁰, L. Pontecorvo^{132a}, B.G. Pope⁹⁰, G.A. Popeneciu^{26b}, D.S. Popovic¹³, A. Poppleton³⁰, S. Pospisil¹²⁸, K. Potamianos¹⁵, I.N. Potrap⁶⁵, C.J. Potter¹⁴⁹, C.T. Potter¹¹⁶, G. Poulard³⁰, J. Poveda³⁰, V. Pozdnyakov⁶⁵, P. Pralavorio⁸⁵, A. Pranko¹⁵, S. Prasad³⁰, S. Prell⁶⁴, D. Price⁸⁴, L.E. Price⁶, M. Primavera^{73a}, S. Prince⁸⁷, M. Proissl⁴⁶, K. Prokofiev^{60c}, F. Prokoshin^{32b}, E. Protopapadaki¹³⁶, S. Protopopescu²⁵, J. Proudfoot⁶, M. Przybycien^{38a}, E. Ptacek¹¹⁶, D. Puddu^{134a,134b}, E. Pueschel⁸⁶, D. Puldon¹⁴⁸, M. Purohit^{25,ad}, P. Puzo¹¹⁷, J. Qian⁸⁹, G. Qin⁵³, Y. Qin⁸⁴,

A. Quadt⁵⁴, D.R. Quarrie¹⁵, W.B. Quayle^{164a,164b}, M. Queitsch-Maitland⁸⁴, D. Quilty⁵³, S. Raddum¹¹⁹, V. Radeka²⁵, V. Radescu⁴², S.K. Radhakrishnan¹⁴⁸, P. Radloff¹¹⁶, P. Rados⁸⁸, F. Ragusa^{91a,91b}, G. Rahal¹⁷⁸, S. Rajagopalan²⁵, M. Rammensee³⁰, C. Rangel-Smith¹⁶⁶, F. Rauscher¹⁰⁰, S. Rave⁸³, T. Ravenscroft⁵³, M. Raymond³⁰, A.L. Read¹¹⁹, N.P. Readoff⁷⁴, D.M. Rebuzzi^{121a,121b}, A. Redelbach¹⁷⁴, G. Redlinger²⁵, R. Reece¹³⁷, K. Reeves⁴¹, L. Rehnisch¹⁶, J. Reichert¹²², H. Reisin²⁷, M. Relich¹⁶³, C. Rembser³⁰, H. Ren^{33a}, A. Renaud¹¹⁷, M. Rescigno^{132a}, S. Resconi^{91a}, O.L. Rezanova^{109,c}, P. Reznicek¹²⁹, R. Rezvani⁹⁵, R. Richter¹⁰¹, S. Richter⁷⁸, E. Richter-Was^{38b}, O. Ricken²¹, M. Ridel⁸⁰, P. Rieck¹⁶, C.J. Riegel¹⁷⁵, J. Rieger⁵⁴, M. Rijssenbeek¹⁴⁸, A. Rimoldi^{121a,121b}, L. Rinaldi^{20a}, B. Ristić⁴⁹, E. Ritsch³⁰, I. Riu¹², F. Rizatdinova¹¹⁴, E. Rizvi⁷⁶, S.H. Robertson^{87,k}, A. Robichaud-Veronneau⁸⁷, D. Robinson²⁸, J.E.M. Robinson⁴², A. Robson⁵³, C. Roda^{124a,124b}, S. Roe³⁰, O. Røhne¹¹⁹, S. Rolli¹⁶¹, A. Romaniouk⁹⁸, M. Romano^{20a,20b}, S.M. Romano Saez³⁴, E. Romero Adam¹⁶⁷, N. Rompotis¹³⁸, M. Ronzani⁴⁸, L. Roos⁸⁰, E. Ros¹⁶⁷, S. Rosati^{132a}, K. Rosbach⁴⁸, P. Rose¹³⁷, P.L. Rosendahl¹⁴, O. Rosenthal¹⁴¹, V. Rossetti^{146a,146b}, E. Rossi^{104a,104b}, L.P. Rossi^{50a}, R. Rosten¹³⁸, M. Rotaru^{26a}, I. Roth¹⁷², J. Rothberg¹³⁸, D. Rousseau¹¹⁷, C.R. Royon¹³⁶, A. Rozanov⁸⁵, Y. Rozen¹⁵², X. Ruan^{145c}, F. Rubbo¹⁴³, I. Rubinskiy⁴², V.I. Rud⁹⁹, C. Rudolph⁴⁴, M.S. Rudolph¹⁵⁸, F. Rühr⁴⁸, A. Ruiz-Martinez³⁰, Z. Rurikova⁴⁸, N.A. Rusakovich⁶⁵, A. Ruschke¹⁰⁰, H.L. Russell¹³⁸, J.P. Rutherford⁷, N. Ruthmann⁴⁸, Y.F. Ryabov¹²³, M. Rybar¹⁶⁵, G. Rybkin¹¹⁷, N.C. Ryder¹²⁰, A.F. Saavedra¹⁵⁰, G. Sabato¹⁰⁷, S. Sacerdoti²⁷, A. Saddique³, H.F-W. Sadrozinski¹³⁷, R. Sadykov⁶⁵, F. Safai Tehrani^{132a}, M. Sahinsoy^{19a}, M. Saimpert¹³⁶, T. Saito¹⁵⁵, H. Sakamoto¹⁵⁵, Y. Sakurai¹⁷¹, G. Salamanna^{134a,134b}, A. Salamon^{133a}, M. Saleem¹¹³, D. Salek¹⁰⁷, P.H. Sales De Bruin¹³⁸, D. Salihagic¹⁰¹, A. Salnikov¹⁴³, J. Salt¹⁶⁷, D. Salvatore^{37a,37b}, F. Salvatore¹⁴⁹, A. Salvucci¹⁰⁶, A. Salzburger³⁰, D. Sammel⁴⁸, D. Sampsonidis¹⁵⁴, A. Sanchez^{104a,104b}, J. Sánchez¹⁶⁷, V. Sanchez Martinez¹⁶⁷, H. Sandaker¹¹⁹, R.L. Sandbach⁷⁶, H.G. Sander⁸³, M.P. Sanders¹⁰⁰, M. Sandhoff¹⁷⁵, C. Sandoval¹⁶², R. Sandstroem¹⁰¹, D.P.C. Sankey¹³¹, M. Sannino^{50a,50b}, A. Sansoni⁴⁷, C. Santoni³⁴, R. Santonico^{133a,133b}, H. Santos^{126a}, I. Santoyo Castillo¹⁴⁹, K. Sapp¹²⁵, A. Sapronov⁶⁵, J.G. Saraiva^{126a,126d}, B. Sarrazin²¹, O. Sasaki⁶⁶, Y. Sasaki¹⁵⁵, K. Sato¹⁶⁰, G. Sauvage^{5,*}, E. Sauvan⁵, G. Savage⁷⁷, P. Savard^{158,d}, C. Sawyer¹³¹, L. Sawyer^{79,n}, J. Saxon³¹, C. Sbarra^{20a}, A. Sbrizzi^{20a,20b}, T. Scanlon⁷⁸, D.A. Scannicchio¹⁶³, M. Scarcella¹⁵⁰, V. Scarfone^{37a,37b}, J. Schaarschmidt¹⁷², P. Schacht¹⁰¹, D. Schaefer³⁰, R. Schaefer⁴², J. Schaeffer⁸³, S. Schaepe²¹, S. Schaetzl^{58b}, U. Schäfer⁸³, A.C. Schaffler¹¹⁷, D. Schaile¹⁰⁰, R.D. Schamberger¹⁴⁸, V. Scharf^{58a}, V.A. Schegelsky¹²³, D. Scheirich¹²⁹, M. Schernau¹⁶³, C. Schiavi^{50a,50b}, C. Schillo⁴⁸, M. Schioppa^{37a,37b}, S. Schlenker³⁰, E. Schmidt⁴⁸, K. Schmieden³⁰, C. Schmitt⁸³, S. Schmitt^{58b}, S. Schmitt⁴², B. Schneider^{159a}, Y.J. Schnellbach⁷⁴, U. Schnoor⁴⁴, L. Schoeffel¹³⁶, A. Schoening^{58b}, B.D. Schoenrock⁹⁰, E. Schopf²¹, A.L.S. Schorlemmer⁵⁴, M. Schott⁸³, D. Schouten^{159a}, J. Schovancova⁸, S. Schramm⁴⁹, M. Schreyer¹⁷⁴, C. Schroeder⁸³, N. Schuh⁸³, M.J. Schultens²¹, H.-C. Schultz-Coulon^{58a}, H. Schulz¹⁶, M. Schumacher⁴⁸, B.A. Schumm¹³⁷, Ph. Schune¹³⁶, C. Schwanenberger⁸⁴, A. Schwartzman¹⁴³, T.A. Schwarz⁸⁹, Ph. Schwegler¹⁰¹, H. Schweiger⁸⁴, Ph. Schwemling¹³⁶, R. Schwienhorst⁹⁰, J. Schwindling¹³⁶, T. Schwindt²¹, F.G. Sciacca¹⁷, E. Scifo¹¹⁷, G. Sciolla²³, F. Scuri^{124a,124b}, F. Scutti²¹, J. Searcy⁸⁹, G. Sedov⁴², E. Sedykh¹²³, P. Seema²¹, S.C. Seidel¹⁰⁵, A. Seiden¹³⁷, F. Seifert¹²⁸, J.M. Seixas^{24a}, G. Sekhniadze^{104a}, K. Sekhon⁸⁹, S.J. Sekula⁴⁰, D.M. Seliverstov^{123,*}, N. Semprini-Cesari^{20a,20b}, C. Serfon³⁰, L. Serin¹¹⁷, L. Serkin^{164a,164b}, T. Serre⁸⁵, M. Sessa^{134a,134b}, R. Seuster^{159a}, H. Severini¹¹³, T. Sfiligoj⁷⁵, F. Sforza³⁰, A. Sfyrla³⁰, E. Shabalina⁵⁴, M. Shamim¹¹⁶, L.Y. Shan^{33a}, R. Shang¹⁶⁵, J.T. Shank²², M. Shapiro¹⁵, P.B. Shatalov⁹⁷, K. Shaw^{164a,164b}, S.M. Shaw⁸⁴, A. Shcherbakova^{146a,146b}, C.Y. Shehu¹⁴⁹, P. Sherwood⁷⁸, L. Shi^{151,ae}, S. Shimizu⁶⁷, C.O. Shimmin¹⁶³, M. Shimojima¹⁰², M. Shiyakova⁶⁵, A. Shmeleva⁹⁶, D. Shoaleh Saadi⁹⁵, M.J. Shochet³¹, S. Shojaii^{91a,91b}, S. Shrestha¹¹¹, E. Shulga⁹⁸, M.A. Shupe⁷, S. Shushkevich⁴², P. Sicho¹²⁷, P.E. Sidebo¹⁴⁷, O. Sidiropoulou¹⁷⁴, D. Sidorov¹¹⁴, A. Sidoti^{20a,20b}, F. Siegert⁴⁴, Dj. Sijacki¹³, J. Silva^{126a,126d}, Y. Silver¹⁵³,

S.B. Silverstein^{146a}, V. Simak¹²⁸, O. Simard⁵, Lj. Simic¹³, S. Simion¹¹⁷, E. Simioni⁸³, B. Simmons⁷⁸, D. Simon³⁴, R. Simonello^{91a,91b}, P. Sinervo¹⁵⁸, N.B. Sinev¹¹⁶, M. Sioli^{20a,20b}, G. Siragusa¹⁷⁴, A.N. Sisakyan^{65,*}, S.Yu. Sivoklokov⁹⁹, J. Sjölin^{146a,146b}, T.B. Sjursen¹⁴, M.B. Skinner⁷², H.P. Skottowe⁵⁷, P. Skubic¹¹³, M. Slater¹⁸, T. Slavicek¹²⁸, M. Slawinska¹⁰⁷, K. Sliwa¹⁶¹, V. Smakhtin¹⁷², B.H. Smart⁴⁶, L. Smestad¹⁴, S.Yu. Smirnov⁹⁸, Y. Smirnov⁹⁸, L.N. Smirnova^{99,af}, O. Smirnova⁸¹, M.N.K. Smith³⁵, R.W. Smith³⁵, M. Smizanska⁷², K. Smolek¹²⁸, A.A. Snesarev⁹⁶, G. Snidero⁷⁶, S. Snyder²⁵, R. Sobie^{169,k}, F. Socher⁴⁴, A. Soffer¹⁵³, D.A. Soh^{151,ae}, C.A. Solans³⁰, M. Solar¹²⁸, J. Solc¹²⁸, E.Yu. Soldatov⁹⁸, U. Soldevila¹⁶⁷, A.A. Solodkov¹³⁰, A. Soloshenko⁶⁵, O.V. Solovyanov¹³⁰, V. Solovyev¹²³, P. Sommer⁴⁸, H.Y. Song^{33b}, N. Soni¹, A. Sood¹⁵, A. Sopczak¹²⁸, B. Sopko¹²⁸, V. Sopko¹²⁸, V. Sorin¹², D. Sosa^{58b}, M. Sosebee⁸, C.L. Sotiropoulou^{124a,124b}, R. Soualah^{164a,164c}, A.M. Soukharev^{109,c}, D. South⁴², B.C. Sowden⁷⁷, S. Spagnolo^{73a,73b}, M. Spalla^{124a,124b}, F. Spanò⁷⁷, W.R. Spearman⁵⁷, D. Sperlich¹⁶, F. Spettel¹⁰¹, R. Spighi^{20a}, G. Spigo³⁰, L.A. Spiller⁸⁸, M. Spousta¹²⁹, T. Spreitzer¹⁵⁸, R.D. St. Denis^{53,*}, S. Staerz⁴⁴, J. Stahlman¹²², R. Stamen^{58a}, S. Stamm¹⁶, E. Stanecka³⁹, C. Stanescu^{134a}, M. Stanescu-Bellu⁴², M.M. Stanitzki⁴², S. Stapnes¹¹⁹, E.A. Starchenko¹³⁰, J. Stark⁵⁵, P. Staroba¹²⁷, P. Starovoitov⁴², R. Staszewski³⁹, P. Stavina^{144a,*}, P. Steinberg²⁵, B. Stelzer¹⁴², H.J. Stelzer³⁰, O. Stelzer-Chilton^{159a}, H. Stenzel⁵², G.A. Stewart⁵³, J.A. Stillings²¹, M.C. Stockton⁸⁷, M. Stoebe⁸⁷, G. Stoica^{26a}, P. Stolte⁵⁴, S. Stonjek¹⁰¹, A.R. Stradling⁸, A. Straessner⁴⁴, M.E. Stramaglia¹⁷, J. Strandberg¹⁴⁷, S. Strandberg^{146a,146b}, A. Strandlie¹¹⁹, E. Strauss¹⁴³, M. Strauss¹¹³, P. Strizenec^{144b}, R. Ströhmer¹⁷⁴, D.M. Strom¹¹⁶, R. Stroynowski⁴⁰, A. Strubig¹⁰⁶, S.A. Stucci¹⁷, B. Stugu¹⁴, N.A. Styles⁴², D. Su¹⁴³, J. Su¹²⁵, R. Subramaniam⁷⁹, A. Succurro¹², Y. Sugaya¹¹⁸, C. Suhr¹⁰⁸, M. Suk¹²⁸, V.V. Sulin⁹⁶, S. Sultansoy^{4c}, T. Sumida⁶⁸, S. Sun⁵⁷, X. Sun^{33a}, J.E. Sundermann⁴⁸, K. Suruliz¹⁴⁹, G. Susinno^{37a,37b}, M.R. Sutton¹⁴⁹, S. Suzuki⁶⁶, M. Svatos¹²⁷, S. Swedish¹⁶⁸, M. Swiatlowski¹⁴³, I. Sykora^{144a}, T. Sykora¹²⁹, D. Ta⁹⁰, C. Taccini^{134a,134b}, K. Tackmann⁴², J. Taenzer¹⁵⁸, A. Taffard¹⁶³, R. Tafirout^{159a}, N. Taiblum¹⁵³, H. Takai²⁵, R. Takashima⁶⁹, H. Takeda⁶⁷, T. Takeshita¹⁴⁰, Y. Takubo⁶⁶, M. Talby⁸⁵, A.A. Talyshев^{109,c}, J.Y.C. Tam¹⁷⁴, K.G. Tan⁸⁸, J. Tanaka¹⁵⁵, R. Tanaka¹¹⁷, S. Tanaka⁶⁶, B.B. Tannenwald¹¹¹, N. Tannoury²¹, S. Tapprogge⁸³, S. Tarem¹⁵², F. Tarrade²⁹, G.F. Tartarelli^{91a}, P. Tas¹²⁹, M. Tasevsky¹²⁷, T. Tashiro⁶⁸, E. Tassi^{37a,37b}, A. Tavares Delgado^{126a,126b}, Y. Tayalati^{135d}, F.E. Taylor⁹⁴, G.N. Taylor⁸⁸, W. Taylor^{159b}, F.A. Teischinger³⁰, M. Teixeira Dias Castanheira⁷⁶, P. Teixeira-Dias⁷⁷, K.K. Temming⁴⁸, H. Ten Kate³⁰, P.K. Teng¹⁵¹, J.J. Teoh¹¹⁸, F. Tepel¹⁷⁵, S. Terada⁶⁶, K. Terashi¹⁵⁵, J. Terron⁸², S. Terzo¹⁰¹, M. Testa⁴⁷, R.J. Teuscher^{158,k}, T. Theveneaux-Pelzer³⁴, J.P. Thomas¹⁸, J. Thomas-Wilsker⁷⁷, E.N. Thompson³⁵, P.D. Thompson¹⁸, R.J. Thompson⁸⁴, A.S. Thompson⁵³, L.A. Thomsen¹⁷⁶, E. Thomson¹²², M. Thomson²⁸, R.P. Thun^{89,*}, M.J. Tibbetts¹⁵, R.E. Ticse Torres⁸⁵, V.O. Tikhomirov^{96,ag}, Yu.A. Tikhonov^{109,c}, S. Timoshenko⁹⁸, E. Tiouchichine⁸⁵, P. Tipton¹⁷⁶, S. Tisserant⁸⁵, K. Todome¹⁵⁷, T. Todorov^{5,*}, S. Todorova-Nova¹²⁹, J. Tojo⁷⁰, S. Tokár^{144a}, K. Tokushuku⁶⁶, K. Tollefson⁹⁰, E. Tolley⁵⁷, L. Tomlinson⁸⁴, M. Tomoto¹⁰³, L. Tompkins^{143,ah}, K. Toms¹⁰⁵, E. Torrence¹¹⁶, H. Torres¹⁴², E. Torró Pastor¹⁶⁷, J. Toth^{85,ai}, F. Touchard⁸⁵, D.R. Tovey¹³⁹, T. Trefzger¹⁷⁴, L. Tremblet³⁰, A. Tricoli³⁰, I.M. Trigger^{159a}, S. Trincaz-Duvold⁸⁰, M.F. Tripiana¹², W. Trischuk¹⁵⁸, B. Trocmé⁵⁵, C. Troncon^{91a}, M. Trottier-McDonald¹⁵, M. Trovatelli¹⁶⁹, P. True⁹⁰, L. Truong^{164a,164c}, M. Trzebinski³⁹, A. Trzupek³⁹, C. Tsarouchas³⁰, J.C-L. Tseng¹²⁰, P.V. Tsiareshka⁹², D. Tsionou¹⁵⁴, G. Tsipolitis¹⁰, N. Tsirintanis⁹, S. Tsiskaridze¹², V. Tsiskaridze⁴⁸, E.G. Tskhadadze^{51a}, I.I. Tsukerman⁹⁷, V. Tsulaia¹⁵, S. Tsuno⁶⁶, D. Tsybychev¹⁴⁸, A. Tudorache^{26a}, V. Tudorache^{26a}, A.N. Tuna¹²², S.A. Tupputi^{20a,20b}, S. Turchikhin^{99,af}, D. Turecek¹²⁸, R. Turra^{91a,91b}, A.J. Turvey⁴⁰, P.M. Tuts³⁵, A. Tykhonov⁴⁹, M. Tylmad^{146a,146b}, M. Tyndel¹³¹, I. Ueda¹⁵⁵, R. Ueno²⁹, M. Ughetto^{146a,146b}, M. Ugland¹⁴, M. Uhlenbrock²¹, F. Ukegawa¹⁶⁰, G. Unal³⁰, A. Undrus²⁵, G. Unel¹⁶³, F.C. Ungaro⁴⁸, Y. Unno⁶⁶, C. Unverdorben¹⁰⁰, J. Urban^{144b}, P. Urquijo⁸⁸, P. Urrejola⁸³, G. Usai⁸, A. Usanova⁶², L. Vacavant⁸⁵, V. Vacek¹²⁸, B. Vachon⁸⁷, C. Valderanis⁸³, N. Valencic¹⁰⁷, S. Valentinetto^{20a,20b}, A. Valero¹⁶⁷,

L. Valery¹², S. Valkar¹²⁹, E. Valladolid Gallego¹⁶⁷, S. Vallecorsa⁴⁹, J.A. Valls Ferrer¹⁶⁷,
 W. Van Den Wollenberg¹⁰⁷, P.C. Van Der Deijl¹⁰⁷, R. van der Geer¹⁰⁷, H. van der Graaf¹⁰⁷,
 R. Van Der Leeuw¹⁰⁷, N. van Eldik¹⁵², P. van Gemmeren⁶, J. Van Nieuwkoop¹⁴², I. van Vulpen¹⁰⁷,
 M.C. van Woerden³⁰, M. Vanadia^{132a,132b}, W. Vandelli³⁰, R. Vanguri¹²², A. Vaniachine⁶, F. Vannucci⁸⁰,
 G. Vardanyan¹⁷⁷, R. Vari^{132a}, E.W. Varnes⁷, T. Varol⁴⁰, D. Varouchas⁸⁰, A. Vartapetian⁸, K.E. Varvell¹⁵⁰,
 F. Vazeille³⁴, T. Vazquez Schroeder⁸⁷, J. Veatch⁷, L.M. Veloce¹⁵⁸, F. Veloso^{126a,126c}, T. Velz²¹,
 S. Veneziano^{132a}, A. Ventura^{73a,73b}, D. Ventura⁸⁶, M. Venturi¹⁶⁹, N. Venturi¹⁵⁸, A. Venturini²³,
 V. Vercesi^{121a}, M. Verducci^{132a,132b}, W. Verkerke¹⁰⁷, J.C. Vermeulen¹⁰⁷, A. Vest⁴⁴, M.C. Vetterli^{142,d},
 O. Viazlo⁸¹, I. Vichou¹⁶⁵, T. Vickey¹³⁹, O.E. Vickey Boeriu¹³⁹, G.H.A. Viehhauser¹²⁰, S. Viel¹⁵,
 R. Vigne⁶², M. Villa^{20a,20b}, M. Villaplana Perez^{91a,91b}, E. Vilucchi⁴⁷, M.G. Vincter²⁹, V.B. Vinogradov⁶⁵,
 I. Vivarelli¹⁴⁹, F. Vives Vaque³, S. Vlachos¹⁰, D. Vladoiu¹⁰⁰, M. Vlasak¹²⁸, M. Vogel^{32a}, P. Vokac¹²⁸,
 G. Volpi^{124a,124b}, M. Volpi⁸⁸, H. von der Schmitt¹⁰¹, H. von Radziewski⁴⁸, E. von Toerne²¹,
 V. Vorobel¹²⁹, K. Vorobev⁹⁸, M. Vos¹⁶⁷, R. Voss³⁰, J.H. Vossebeld⁷⁴, N. Vranjes¹³,
 M. Vranjes Milosavljevic¹³, V. Vrba¹²⁷, M. Vreeswijk¹⁰⁷, R. Vuillermet³⁰, I. Vukotic³¹, Z. Vykydal¹²⁸,
 P. Wagner²¹, W. Wagner¹⁷⁵, H. Wahlberg⁷¹, S. Wahrmund⁴⁴, J. Wakabayashi¹⁰³, J. Walder⁷²,
 R. Walker¹⁰⁰, W. Walkowiak¹⁴¹, C. Wang¹⁵¹, F. Wang¹⁷³, H. Wang¹⁵, H. Wang⁴⁰, J. Wang⁴², J. Wang^{33a},
 K. Wang⁸⁷, R. Wang⁶, S.M. Wang¹⁵¹, T. Wang²¹, T. Wang³⁵, X. Wang¹⁷⁶, C. Wanotayaroj¹¹⁶,
 A. Warburton⁸⁷, C.P. Ward²⁸, D.R. Wardrop⁷⁸, M. Warsinsky⁴⁸, A. Washbrook⁴⁶, C. Wasicki⁴²,
 P.M. Watkins¹⁸, A.T. Watson¹⁸, I.J. Watson¹⁵⁰, M.F. Watson¹⁸, G. Watts¹³⁸, S. Watts⁸⁴, B.M. Waugh⁷⁸,
 S. Webb⁸⁴, M.S. Weber¹⁷, S.W. Weber¹⁷⁴, J.S. Webster³¹, A.R. Weidberg¹²⁰, B. Weinert⁶¹,
 J. Weingarten⁵⁴, C. Weiser⁴⁸, H. Weits¹⁰⁷, P.S. Wells³⁰, T. Wenaus²⁵, T. Wengler³⁰, S. Wenig³⁰,
 N. Wermes²¹, M. Werner⁴⁸, P. Werner³⁰, M. Wessels^{58a}, J. Wetter¹⁶¹, K. Whalen¹¹⁶, A.M. Wharton⁷²,
 A. White⁸, M.J. White¹, R. White^{32b}, S. White^{124a,124b}, D. Whiteson¹⁶³, F.J. Wickens¹³¹,
 W. Wiedenmann¹⁷³, M. Wielers¹³¹, P. Wienemann²¹, C. Wiglesworth³⁶, L.A.M. Wiik-Fuchs²¹,
 A. Wildauer¹⁰¹, H.G. Wilkens³⁰, H.H. Williams¹²², S. Williams¹⁰⁷, C. Willis⁹⁰, S. Willocq⁸⁶,
 A. Wilson⁸⁹, J.A. Wilson¹⁸, I. Wingerter-Seez⁵, F. Winklmeier¹¹⁶, B.T. Winter²¹, M. Wittgen¹⁴³,
 J. Wittkowski¹⁰⁰, S.J. Wollstadt⁸³, M.W. Wolter³⁹, H. Wolters^{126a,126c}, B.K. Wosiek³⁹, J. Wotschack³⁰,
 M.J. Woudstra⁸⁴, K.W. Wozniak³⁹, M. Wu⁵⁵, M. Wu³¹, S.L. Wu¹⁷³, X. Wu⁴⁹, Y. Wu⁸⁹, T.R. Wyatt⁸⁴,
 B.M. Wynne⁴⁶, S. Xella³⁶, D. Xu^{33a}, L. Xu^{33b,aj}, B. Yabsley¹⁵⁰, S. Yacoob^{145a}, R. Yakabe⁶⁷,
 M. Yamada⁶⁶, Y. Yamaguchi¹¹⁸, A. Yamamoto⁶⁶, S. Yamamoto¹⁵⁵, T. Yamanaka¹⁵⁵, K. Yamauchi¹⁰³,
 Y. Yamazaki⁶⁷, Z. Yan²², H. Yang^{33e}, H. Yang¹⁷³, Y. Yang¹⁵¹, W-M. Yao¹⁵, Y. Yasu⁶⁶, E. Yatsenko⁵,
 K.H. Yau Wong²¹, J. Ye⁴⁰, S. Ye²⁵, I. Yeletskikh⁶⁵, A.L. Yen⁵⁷, E. Yildirim⁴², K. Yorita¹⁷¹, R. Yoshida⁶,
 K. Yoshihara¹²², C. Young¹⁴³, C.J.S. Young³⁰, S. Youssef²², D.R. Yu¹⁵, J. Yu⁸, J.M. Yu⁸⁹, J. Yu¹¹⁴,
 L. Yuan⁶⁷, S.P.Y. Yuen²¹, A. Yurkewicz¹⁰⁸, I. Yusuff^{28,ak}, B. Zabinski³⁹, R. Zaidan⁶³, A.M. Zaitsev^{130,aa},
 J. Zalieckas¹⁴, A. Zaman¹⁴⁸, S. Zambito⁵⁷, L. Zanello^{132a,132b}, D. Zanzi⁸⁸, C. Zeitnitz¹⁷⁵, M. Zeman¹²⁸,
 A. Zemla^{38a}, K. Zengel²³, O. Zenin¹³⁰, T. Ženiš^{144a}, D. Zerwas¹¹⁷, D. Zhang⁸⁹, F. Zhang¹⁷³,
 H. Zhang^{33c}, J. Zhang⁶, L. Zhang⁴⁸, R. Zhang^{33b}, X. Zhang^{33d}, Z. Zhang¹¹⁷, X. Zhao⁴⁰, Y. Zhao^{33d,117},
 Z. Zhao^{33b}, A. Zhemchugov⁶⁵, J. Zhong¹²⁰, B. Zhou⁸⁹, C. Zhou⁴⁵, L. Zhou³⁵, L. Zhou⁴⁰, N. Zhou¹⁶³,
 C.G. Zhu^{33d}, H. Zhu^{33a}, J. Zhu⁸⁹, Y. Zhu^{33b}, X. Zhuang^{33a}, K. Zhukov⁹⁶, A. Zibell¹⁷⁴, D. Ziemska⁶¹,
 N.I. Zimine⁶⁵, C. Zimmermann⁸³, S. Zimmermann⁴⁸, Z. Zinonos⁵⁴, M. Zinser⁸³, M. Ziolkowski¹⁴¹,
 L. Živković¹³, G. Zobernig¹⁷³, A. Zoccoli^{20a,20b}, M. zur Nedden¹⁶, G. Zurzolo^{104a,104b}, L. Zwalinski³⁰.

¹ Department of Physics, University of Adelaide, Adelaide, Australia

² Physics Department, SUNY Albany, Albany NY, United States of America

³ Department of Physics, University of Alberta, Edmonton AB, Canada

⁴ ^(a) Department of Physics, Ankara University, Ankara; ^(b) Istanbul Aydin University, Istanbul; ^(c) Division of Physics, TOBB University of Economics and Technology, Ankara, Turkey

- ⁵ LAPP, CNRS/IN2P3 and Université Savoie Mont Blanc, Annecy-le-Vieux, France
⁶ High Energy Physics Division, Argonne National Laboratory, Argonne IL, United States of America
⁷ Department of Physics, University of Arizona, Tucson AZ, United States of America
⁸ Department of Physics, The University of Texas at Arlington, Arlington TX, United States of America
⁹ Physics Department, University of Athens, Athens, Greece
¹⁰ Physics Department, National Technical University of Athens, Zografou, Greece
¹¹ Institute of Physics, Azerbaijan Academy of Sciences, Baku, Azerbaijan
¹² Institut de Física d'Altes Energies and Departament de Física de la Universitat Autònoma de Barcelona, Barcelona, Spain
¹³ Institute of Physics, University of Belgrade, Belgrade, Serbia
¹⁴ Department for Physics and Technology, University of Bergen, Bergen, Norway
¹⁵ Physics Division, Lawrence Berkeley National Laboratory and University of California, Berkeley CA, United States of America
¹⁶ Department of Physics, Humboldt University, Berlin, Germany
¹⁷ Albert Einstein Center for Fundamental Physics and Laboratory for High Energy Physics, University of Bern, Bern, Switzerland
¹⁸ School of Physics and Astronomy, University of Birmingham, Birmingham, United Kingdom
¹⁹ ^(a) Department of Physics, Bogazici University, Istanbul; ^(b) Department of Physics Engineering, Gaziantep University, Gaziantep; ^(c) Department of Physics, Dogus University, Istanbul, Turkey
²⁰ ^(a) INFN Sezione di Bologna; ^(b) Dipartimento di Fisica e Astronomia, Università di Bologna, Bologna, Italy
²¹ Physikalisches Institut, University of Bonn, Bonn, Germany
²² Department of Physics, Boston University, Boston MA, United States of America
²³ Department of Physics, Brandeis University, Waltham MA, United States of America
²⁴ ^(a) Universidade Federal do Rio De Janeiro COPPE/EE/IF, Rio de Janeiro; ^(b) Electrical Circuits Department, Federal University of Juiz de Fora (UFJF), Juiz de Fora; ^(c) Federal University of Sao Joao del Rei (UFSJ), Sao Joao del Rei; ^(d) Instituto de Fisica, Universidade de Sao Paulo, Sao Paulo, Brazil
²⁵ Physics Department, Brookhaven National Laboratory, Upton NY, United States of America
²⁶ ^(a) National Institute of Physics and Nuclear Engineering, Bucharest; ^(b) National Institute for Research and Development of Isotopic and Molecular Technologies, Physics Department, Cluj Napoca; ^(c) University Politehnica Bucharest, Bucharest; ^(d) West University in Timisoara, Timisoara, Romania
²⁷ Departamento de Física, Universidad de Buenos Aires, Buenos Aires, Argentina
²⁸ Cavendish Laboratory, University of Cambridge, Cambridge, United Kingdom
²⁹ Department of Physics, Carleton University, Ottawa ON, Canada
³⁰ CERN, Geneva, Switzerland
³¹ Enrico Fermi Institute, University of Chicago, Chicago IL, United States of America
³² ^(a) Departamento de Física, Pontificia Universidad Católica de Chile, Santiago; ^(b) Departamento de Física, Universidad Técnica Federico Santa María, Valparaíso, Chile
³³ ^(a) Institute of High Energy Physics, Chinese Academy of Sciences, Beijing; ^(b) Department of Modern Physics, University of Science and Technology of China, Anhui; ^(c) Department of Physics, Nanjing University, Jiangsu; ^(d) School of Physics, Shandong University, Shandong; ^(e) Department of Physics and Astronomy, Shanghai Key Laboratory for Particle Physics and Cosmology, Shanghai Jiao Tong University, Shanghai; ^(f) Physics Department, Tsinghua University, Beijing 100084, China
³⁴ Laboratoire de Physique Corpusculaire, Clermont Université and Université Blaise Pascal and CNRS/IN2P3, Clermont-Ferrand, France
³⁵ Nevis Laboratory, Columbia University, Irvington NY, United States of America
³⁶ Niels Bohr Institute, University of Copenhagen, Kobenhavn, Denmark

- ³⁷ ^(a) INFN Gruppo Collegato di Cosenza, Laboratori Nazionali di Frascati; ^(b) Dipartimento di Fisica, Università della Calabria, Rende, Italy
³⁸ ^(a) AGH University of Science and Technology, Faculty of Physics and Applied Computer Science, Krakow; ^(b) Marian Smoluchowski Institute of Physics, Jagiellonian University, Krakow, Poland
³⁹ Institute of Nuclear Physics Polish Academy of Sciences, Krakow, Poland
⁴⁰ Physics Department, Southern Methodist University, Dallas TX, United States of America
⁴¹ Physics Department, University of Texas at Dallas, Richardson TX, United States of America
⁴² DESY, Hamburg and Zeuthen, Germany
⁴³ Institut für Experimentelle Physik IV, Technische Universität Dortmund, Dortmund, Germany
⁴⁴ Institut für Kern- und Teilchenphysik, Technische Universität Dresden, Dresden, Germany
⁴⁵ Department of Physics, Duke University, Durham NC, United States of America
⁴⁶ SUPA - School of Physics and Astronomy, University of Edinburgh, Edinburgh, United Kingdom
⁴⁷ INFN Laboratori Nazionali di Frascati, Frascati, Italy
⁴⁸ Fakultät für Mathematik und Physik, Albert-Ludwigs-Universität, Freiburg, Germany
⁴⁹ Section de Physique, Université de Genève, Geneva, Switzerland
⁵⁰ ^(a) INFN Sezione di Genova; ^(b) Dipartimento di Fisica, Università di Genova, Genova, Italy
⁵¹ ^(a) E. Andronikashvili Institute of Physics, Iv. Javakhishvili Tbilisi State University, Tbilisi; ^(b) High Energy Physics Institute, Tbilisi State University, Tbilisi, Georgia
⁵² II Physikalisches Institut, Justus-Liebig-Universität Giessen, Giessen, Germany
⁵³ SUPA - School of Physics and Astronomy, University of Glasgow, Glasgow, United Kingdom
⁵⁴ II Physikalisches Institut, Georg-August-Universität, Göttingen, Germany
⁵⁵ Laboratoire de Physique Subatomique et de Cosmologie, Université Grenoble-Alpes, CNRS/IN2P3, Grenoble, France
⁵⁶ Department of Physics, Hampton University, Hampton VA, United States of America
⁵⁷ Laboratory for Particle Physics and Cosmology, Harvard University, Cambridge MA, United States of America
⁵⁸ ^(a) Kirchhoff-Institut für Physik, Ruprecht-Karls-Universität Heidelberg, Heidelberg; ^(b) Physikalisches Institut, Ruprecht-Karls-Universität Heidelberg, Heidelberg; ^(c) ZITI Institut für technische Informatik, Ruprecht-Karls-Universität Heidelberg, Mannheim, Germany
⁵⁹ Faculty of Applied Information Science, Hiroshima Institute of Technology, Hiroshima, Japan
⁶⁰ ^(a) Department of Physics, The Chinese University of Hong Kong, Shatin, N.T., Hong Kong; ^(b) Department of Physics, The University of Hong Kong, Hong Kong; ^(c) Department of Physics, The Hong Kong University of Science and Technology, Clear Water Bay, Kowloon, Hong Kong, China
⁶¹ Department of Physics, Indiana University, Bloomington IN, United States of America
⁶² Institut für Astro- und Teilchenphysik, Leopold-Franzens-Universität, Innsbruck, Austria
⁶³ University of Iowa, Iowa City IA, United States of America
⁶⁴ Department of Physics and Astronomy, Iowa State University, Ames IA, United States of America
⁶⁵ Joint Institute for Nuclear Research, JINR Dubna, Dubna, Russia
⁶⁶ KEK, High Energy Accelerator Research Organization, Tsukuba, Japan
⁶⁷ Graduate School of Science, Kobe University, Kobe, Japan
⁶⁸ Faculty of Science, Kyoto University, Kyoto, Japan
⁶⁹ Kyoto University of Education, Kyoto, Japan
⁷⁰ Department of Physics, Kyushu University, Fukuoka, Japan
⁷¹ Instituto de Física La Plata, Universidad Nacional de La Plata and CONICET, La Plata, Argentina
⁷² Physics Department, Lancaster University, Lancaster, United Kingdom
⁷³ ^(a) INFN Sezione di Lecce; ^(b) Dipartimento di Matematica e Fisica, Università del Salento, Lecce, Italy

- ⁷⁴ Oliver Lodge Laboratory, University of Liverpool, Liverpool, United Kingdom
⁷⁵ Department of Physics, Jožef Stefan Institute and University of Ljubljana, Ljubljana, Slovenia
⁷⁶ School of Physics and Astronomy, Queen Mary University of London, London, United Kingdom
⁷⁷ Department of Physics, Royal Holloway University of London, Surrey, United Kingdom
⁷⁸ Department of Physics and Astronomy, University College London, London, United Kingdom
⁷⁹ Louisiana Tech University, Ruston LA, United States of America
⁸⁰ Laboratoire de Physique Nucléaire et de Hautes Energies, UPMC and Université Paris-Diderot and CNRS/IN2P3, Paris, France
⁸¹ Fysiska institutionen, Lunds universitet, Lund, Sweden
⁸² Departamento de Fisica Teorica C-15, Universidad Autonoma de Madrid, Madrid, Spain
⁸³ Institut für Physik, Universität Mainz, Mainz, Germany
⁸⁴ School of Physics and Astronomy, University of Manchester, Manchester, United Kingdom
⁸⁵ CPPM, Aix-Marseille Université and CNRS/IN2P3, Marseille, France
⁸⁶ Department of Physics, University of Massachusetts, Amherst MA, United States of America
⁸⁷ Department of Physics, McGill University, Montreal QC, Canada
⁸⁸ School of Physics, University of Melbourne, Victoria, Australia
⁸⁹ Department of Physics, The University of Michigan, Ann Arbor MI, United States of America
⁹⁰ Department of Physics and Astronomy, Michigan State University, East Lansing MI, United States of America
⁹¹ ^(a) INFN Sezione di Milano; ^(b) Dipartimento di Fisica, Università di Milano, Milano, Italy
⁹² B.I. Stepanov Institute of Physics, National Academy of Sciences of Belarus, Minsk, Republic of Belarus
⁹³ National Scientific and Educational Centre for Particle and High Energy Physics, Minsk, Republic of Belarus
⁹⁴ Department of Physics, Massachusetts Institute of Technology, Cambridge MA, United States of America
⁹⁵ Group of Particle Physics, University of Montreal, Montreal QC, Canada
⁹⁶ P.N. Lebedev Institute of Physics, Academy of Sciences, Moscow, Russia
⁹⁷ Institute for Theoretical and Experimental Physics (ITEP), Moscow, Russia
⁹⁸ National Research Nuclear University MEPhI, Moscow, Russia
⁹⁹ D.V. Skobeltsyn Institute of Nuclear Physics, M.V. Lomonosov Moscow State University, Moscow, Russia
¹⁰⁰ Fakultät für Physik, Ludwig-Maximilians-Universität München, München, Germany
¹⁰¹ Max-Planck-Institut für Physik (Werner-Heisenberg-Institut), München, Germany
¹⁰² Nagasaki Institute of Applied Science, Nagasaki, Japan
¹⁰³ Graduate School of Science and Kobayashi-Maskawa Institute, Nagoya University, Nagoya, Japan
¹⁰⁴ ^(a) INFN Sezione di Napoli; ^(b) Dipartimento di Fisica, Università di Napoli, Napoli, Italy
¹⁰⁵ Department of Physics and Astronomy, University of New Mexico, Albuquerque NM, United States of America
¹⁰⁶ Institute for Mathematics, Astrophysics and Particle Physics, Radboud University Nijmegen/Nikhef, Nijmegen, Netherlands
¹⁰⁷ Nikhef National Institute for Subatomic Physics and University of Amsterdam, Amsterdam, Netherlands
¹⁰⁸ Department of Physics, Northern Illinois University, DeKalb IL, United States of America
¹⁰⁹ Budker Institute of Nuclear Physics, SB RAS, Novosibirsk, Russia
¹¹⁰ Department of Physics, New York University, New York NY, United States of America
¹¹¹ Ohio State University, Columbus OH, United States of America

- ¹¹² Faculty of Science, Okayama University, Okayama, Japan
¹¹³ Homer L. Dodge Department of Physics and Astronomy, University of Oklahoma, Norman OK, United States of America
¹¹⁴ Department of Physics, Oklahoma State University, Stillwater OK, United States of America
¹¹⁵ Palacký University, RCPTM, Olomouc, Czech Republic
¹¹⁶ Center for High Energy Physics, University of Oregon, Eugene OR, United States of America
¹¹⁷ LAL, Université Paris-Sud and CNRS/IN2P3, Orsay, France
¹¹⁸ Graduate School of Science, Osaka University, Osaka, Japan
¹¹⁹ Department of Physics, University of Oslo, Oslo, Norway
¹²⁰ Department of Physics, Oxford University, Oxford, United Kingdom
¹²¹ ^(a) INFN Sezione di Pavia; ^(b) Dipartimento di Fisica, Università di Pavia, Pavia, Italy
¹²² Department of Physics, University of Pennsylvania, Philadelphia PA, United States of America
¹²³ National Research Centre "Kurchatov Institute" B.P.Konstantinov Petersburg Nuclear Physics Institute, St. Petersburg, Russia
¹²⁴ ^(a) INFN Sezione di Pisa; ^(b) Dipartimento di Fisica E. Fermi, Università di Pisa, Pisa, Italy
¹²⁵ Department of Physics and Astronomy, University of Pittsburgh, Pittsburgh PA, United States of America
¹²⁶ ^(a) Laboratório de Instrumentação e Física Experimental de Partículas - LIP, Lisboa; ^(b) Faculdade de Ciências, Universidade de Lisboa, Lisboa; ^(c) Department of Physics, University of Coimbra, Coimbra; ^(d) Centro de Física Nuclear da Universidade de Lisboa, Lisboa; ^(e) Departamento de Física, Universidade do Minho, Braga; ^(f) Departamento de Física Teórica y del Cosmos and CAFPE, Universidad de Granada, Granada (Spain); ^(g) Dep Física and CEFITEC of Faculdade de Ciencias e Tecnologia, Universidade Nova de Lisboa, Caparica, Portugal
¹²⁷ Institute of Physics, Academy of Sciences of the Czech Republic, Praha, Czech Republic
¹²⁸ Czech Technical University in Prague, Praha, Czech Republic
¹²⁹ Faculty of Mathematics and Physics, Charles University in Prague, Praha, Czech Republic
¹³⁰ State Research Center Institute for High Energy Physics, Protvino, Russia
¹³¹ Particle Physics Department, Rutherford Appleton Laboratory, Didcot, United Kingdom
¹³² ^(a) INFN Sezione di Roma; ^(b) Dipartimento di Fisica, Sapienza Università di Roma, Roma, Italy
¹³³ ^(a) INFN Sezione di Roma Tor Vergata; ^(b) Dipartimento di Fisica, Università di Roma Tor Vergata, Roma, Italy
¹³⁴ ^(a) INFN Sezione di Roma Tre; ^(b) Dipartimento di Matematica e Fisica, Università Roma Tre, Roma, Italy
¹³⁵ ^(a) Faculté des Sciences Ain Chock, Réseau Universitaire de Physique des Hautes Energies - Université Hassan II, Casablanca; ^(b) Centre National de l'Energie des Sciences Techniques Nucléaires, Rabat; ^(c) Faculté des Sciences Semlalia, Université Cadi Ayyad, LPHEA-Marrakech; ^(d) Faculté des Sciences, Université Mohamed Premier and LPTPM, Oujda; ^(e) Faculté des sciences, Université Mohammed V-Agdal, Rabat, Morocco
¹³⁶ DSM/IRFU (Institut de Recherches sur les Lois Fondamentales de l'Univers), CEA Saclay (Commissariat à l'Energie Atomique et aux Energies Alternatives), Gif-sur-Yvette, France
¹³⁷ Santa Cruz Institute for Particle Physics, University of California Santa Cruz, Santa Cruz CA, United States of America
¹³⁸ Department of Physics, University of Washington, Seattle WA, United States of America
¹³⁹ Department of Physics and Astronomy, University of Sheffield, Sheffield, United Kingdom
¹⁴⁰ Department of Physics, Shinshu University, Nagano, Japan
¹⁴¹ Fachbereich Physik, Universität Siegen, Siegen, Germany
¹⁴² Department of Physics, Simon Fraser University, Burnaby BC, Canada

- ¹⁴³ SLAC National Accelerator Laboratory, Stanford CA, United States of America
- ¹⁴⁴ ^(a) Faculty of Mathematics, Physics & Informatics, Comenius University, Bratislava; ^(b) Department of Subnuclear Physics, Institute of Experimental Physics of the Slovak Academy of Sciences, Kosice, Slovak Republic
- ¹⁴⁵ ^(a) Department of Physics, University of Cape Town, Cape Town; ^(b) Department of Physics, University of Johannesburg, Johannesburg; ^(c) School of Physics, University of the Witwatersrand, Johannesburg, South Africa
- ¹⁴⁶ ^(a) Department of Physics, Stockholm University; ^(b) The Oskar Klein Centre, Stockholm, Sweden
- ¹⁴⁷ Physics Department, Royal Institute of Technology, Stockholm, Sweden
- ¹⁴⁸ Departments of Physics & Astronomy and Chemistry, Stony Brook University, Stony Brook NY, United States of America
- ¹⁴⁹ Department of Physics and Astronomy, University of Sussex, Brighton, United Kingdom
- ¹⁵⁰ School of Physics, University of Sydney, Sydney, Australia
- ¹⁵¹ Institute of Physics, Academia Sinica, Taipei, Taiwan
- ¹⁵² Department of Physics, Technion: Israel Institute of Technology, Haifa, Israel
- ¹⁵³ Raymond and Beverly Sackler School of Physics and Astronomy, Tel Aviv University, Tel Aviv, Israel
- ¹⁵⁴ Department of Physics, Aristotle University of Thessaloniki, Thessaloniki, Greece
- ¹⁵⁵ International Center for Elementary Particle Physics and Department of Physics, The University of Tokyo, Tokyo, Japan
- ¹⁵⁶ Graduate School of Science and Technology, Tokyo Metropolitan University, Tokyo, Japan
- ¹⁵⁷ Department of Physics, Tokyo Institute of Technology, Tokyo, Japan
- ¹⁵⁸ Department of Physics, University of Toronto, Toronto ON, Canada
- ¹⁵⁹ ^(a) TRIUMF, Vancouver BC; ^(b) Department of Physics and Astronomy, York University, Toronto ON, Canada
- ¹⁶⁰ Faculty of Pure and Applied Sciences, University of Tsukuba, Tsukuba, Japan
- ¹⁶¹ Department of Physics and Astronomy, Tufts University, Medford MA, United States of America
- ¹⁶² Centro de Investigaciones, Universidad Antonio Narino, Bogota, Colombia
- ¹⁶³ Department of Physics and Astronomy, University of California Irvine, Irvine CA, United States of America
- ¹⁶⁴ ^(a) INFN Gruppo Collegato di Udine, Sezione di Trieste, Udine; ^(b) ICTP, Trieste; ^(c) Dipartimento di Chimica, Fisica e Ambiente, Università di Udine, Udine, Italy
- ¹⁶⁵ Department of Physics, University of Illinois, Urbana IL, United States of America
- ¹⁶⁶ Department of Physics and Astronomy, University of Uppsala, Uppsala, Sweden
- ¹⁶⁷ Instituto de Física Corpuscular (IFIC) and Departamento de Física Atómica, Molecular y Nuclear and Departamento de Ingeniería Electrónica and Instituto de Microelectrónica de Barcelona (IMB-CNM), University of Valencia and CSIC, Valencia, Spain
- ¹⁶⁸ Department of Physics, University of British Columbia, Vancouver BC, Canada
- ¹⁶⁹ Department of Physics and Astronomy, University of Victoria, Victoria BC, Canada
- ¹⁷⁰ Department of Physics, University of Warwick, Coventry, United Kingdom
- ¹⁷¹ Waseda University, Tokyo, Japan
- ¹⁷² Department of Particle Physics, The Weizmann Institute of Science, Rehovot, Israel
- ¹⁷³ Department of Physics, University of Wisconsin, Madison WI, United States of America
- ¹⁷⁴ Fakultät für Physik und Astronomie, Julius-Maximilians-Universität, Würzburg, Germany
- ¹⁷⁵ Fachbereich C Physik, Bergische Universität Wuppertal, Wuppertal, Germany
- ¹⁷⁶ Department of Physics, Yale University, New Haven CT, United States of America
- ¹⁷⁷ Yerevan Physics Institute, Yerevan, Armenia

- ¹⁷⁸ Centre de Calcul de l’Institut National de Physique Nucléaire et de Physique des Particules (IN2P3), Villeurbanne, France
- ^a Also at Department of Physics, King’s College London, London, United Kingdom
- ^b Also at Institute of Physics, Azerbaijan Academy of Sciences, Baku, Azerbaijan
- ^c Also at Novosibirsk State University, Novosibirsk, Russia
- ^d Also at TRIUMF, Vancouver BC, Canada
- ^e Also at Department of Physics, California State University, Fresno CA, United States of America
- ^f Also at Department of Physics, University of Fribourg, Fribourg, Switzerland
- ^g Also at Departamento de Fisica e Astronomia, Faculdade de Ciencias, Universidade do Porto, Portugal
- ^h Also at Tomsk State University, Tomsk, Russia
- ⁱ Also at CPPM, Aix-Marseille Université and CNRS/IN2P3, Marseille, France
- ^j Also at Universita di Napoli Parthenope, Napoli, Italy
- ^k Also at Institute of Particle Physics (IPP), Canada
- ^l Also at Particle Physics Department, Rutherford Appleton Laboratory, Didcot, United Kingdom
- ^m Also at Department of Physics, St. Petersburg State Polytechnical University, St. Petersburg, Russia
- ⁿ Also at Louisiana Tech University, Ruston LA, United States of America
- ^o Also at Institutio Catalana de Recerca i Estudis Avancats, ICREA, Barcelona, Spain
- ^p Also at Department of Physics, National Tsing Hua University, Taiwan
- ^q Also at Department of Physics, The University of Texas at Austin, Austin TX, United States of America
- ^r Also at Institute of Theoretical Physics, Ilia State University, Tbilisi, Georgia
- ^s Also at CERN, Geneva, Switzerland
- ^t Also at Georgian Technical University (GTU), Tbilisi, Georgia
- ^u Also at Manhattan College, New York NY, United States of America
- ^v Also at Hellenic Open University, Patras, Greece
- ^w Also at Institute of Physics, Academia Sinica, Taipei, Taiwan
- ^x Also at LAL, Université Paris-Sud and CNRS/IN2P3, Orsay, France
- ^y Also at Academia Sinica Grid Computing, Institute of Physics, Academia Sinica, Taipei, Taiwan
- ^z Also at School of Physics, Shandong University, Shandong, China
- ^{aa} Also at Moscow Institute of Physics and Technology State University, Dolgoprudny, Russia
- ^{ab} Also at Section de Physique, Université de Genève, Geneva, Switzerland
- ^{ac} Also at International School for Advanced Studies (SISSA), Trieste, Italy
- ^{ad} Also at Department of Physics and Astronomy, University of South Carolina, Columbia SC, United States of America
- ^{ae} Also at School of Physics and Engineering, Sun Yat-sen University, Guangzhou, China
- ^{af} Also at Faculty of Physics, M.V.Lomonosov Moscow State University, Moscow, Russia
- ^{ag} Also at National Research Nuclear University MEPhI, Moscow, Russia
- ^{ah} Also at Department of Physics, Stanford University, Stanford CA, United States of America
- ^{ai} Also at Institute for Particle and Nuclear Physics, Wigner Research Centre for Physics, Budapest, Hungary
- ^{aj} Also at Department of Physics, The University of Michigan, Ann Arbor MI, United States of America
- ^{ak} Also at University of Malaya, Department of Physics, Kuala Lumpur, Malaysia
- * Deceased